Aus der Neurochirurgischen Klinik und Poliklinik

der Ludwigs-Maximilians-Universität München

Direktor: Prof. Dr. med. Jörg-Christian Tonn

Investigating pericyte progenitor cells in glioma angiogenesis and postnatal brain development

Dissertation

zum Erwerb des Doktorgrades der Medizin

an der Medizinischen Fakultät der

Ludwig-Maximilians-Universität zu München

vorgelegt von

Yingxi Wu

aus Zhengzhou, P.R. China

2018

Mit Genehmigung der Medizinischen Fakultät

der Universität München

Berichterstatter: Prof. Dr. rer. nat. Rainer Glaß

Mitberichterstatter: Prof. Frank Staub

Prof. Jochen Herms

Mitbetreuung durch den

promovierten Mitarbeiter: Dr. sc. nat. Roland Kälin

Dekan: Prof. Dr. med. dent. Reinhard Hickel

Tag der mündlichen Prüfung: 18.01.2018

Eidesstattliche Versicherung

Wu, Yingxi
Name, Vorname

Ich erkläre hiermit an Eides statt,
dass ich die vorliegende Dissertation mit dem Thema

Investigating pericyte progenitor cells in glioma angiogenesis and postnatal brain development

selbständig verfasst, mich außer der angegebenen keiner weiteren Hilfsmittel bedient und alle Erkenntnisse, die aus dem Schrifttum ganz oder annähernd übernommen sind, als solche kenntlich gemacht und nach ihrer Herkunft unter Bezeichnung der Fundstelle einzeln nachgewiesen habe.

Ich erkläre des Weiteren, dass die hier vorgelegte Dissertation nicht in gleicher oder in ähnlicher Form bei einer anderen Stelle zur Erlangung eines akademischen Grades eingereicht wurde.

Zhengzhou China, June.20.2017
Ort, Datum

Yingxi Wu
Unterschrift Doktorandin/Doktorand

I.Contents

II. List of figures

III. List of tables

IV. Abbreviations

BBB	Blood-Brain -Barrier
BRB	Blood-Retina -Barrier
CD	Cluster of Differentiation
Cre	Cyclization Recombination Enzyme
d	Day
DAB	3,3'-Diaminobenzidine
DAPI	4, 6-diamidino-2-phenylindole
DR	diabetic retinopathy
EDTA	Ethylenediaminetetraacetic acid
Fig.	Figure
GBM	Glioblastoma multiforme
GFAP	Glial fibrillary acidic protein
GL261	Murine high-grade astrocytoma cell line
h	hour(s)
HOPE	hepes-glutamic acid buffer-mediated organic solvent protection effect
i.p.	Intraperitoneal
NG2	neuron-glial 2
NSCs	neural stem cells
PDGFR	platelet-derived growth factor receptor
PBS	Phosphate buffered saline
PFA	Paraformaldehyde

P	postnatal
RFP	red fluorescence protein
SMA	smooth muscle actin
VEGF	vascular endothelial growth factor
VWF	Von Willebrand factor
WHO	World Health Organization
wt	wildtype

1. Introduction

1.1 Gliomas

Gliomas are the most common primary brain tumors in the human central nervous system [1] and constitute approximately more than 70% of all brain malignant tumors [2]. According to the World Health Organization (WHO), gliomas are classified into 4 malignant grades (from I to IV) by histological criteria. Glioblastoma multiforme (GBM, WHO grade IV), the most aggressive glioma type, accounts for more than half of gliomas [3]. In the past decades, despite large efforts in surgery, chemotherapy, radiotherapy and tumor biology, there is still no substantial improvement of the overall 5 year survival rate [4].

1.1.1 Symptoms of gliomas

The different affected positions in the central nervous system cause various symptoms of gliomas. Occasionally tumor only causes asymptomatic condition, but mostly tumor can cause symptoms fast when it grows into an huge size. The brain glioma can lead to increased intracranial pressure and eventually result in vomiting, cranial nerve disorders, headaches and seizures [5]. The spinal cord glioma results in numbness, pain or weakness of extremities. The optic nerve glioma can lead to visual loss. Gliomas usually metastasize through the cerebrospinal fluid instead of spreading via the bloodstream, and subsequently produce “drop metastases” in the spinal cord.

1.1.2 Glioblastomas

Glioblastoma (GBM) is an astrocytic tumor and is considered as extremely malignant, there is an incidence rate of 3.19 per 100,000 which occurs in average at an age of 64 years [6]. It represents approximately 15% of primary intracranial tumors and is classified as the Grade IV tumor by World Health Organization [7]. The main histopathological characteristics of GBM are necrosis, cellular polymorphism, microvascular proliferation, and brisk mitotic activity. The whole prognosis of patients who have GBM stays grim, although there are improvements in multi-modal treatment options and imaging techniques. It is estimated that despite maximal treatment, the median duration of survival is only 12 to 18 months. However, patients who have no intervention die shortly after diagnosis [8, 9]. So far, there are only small number of cases with long-term survival or other curative outcomes that have been reported [10, 11].

1.1.3 Glioma therapy

There are different strategies for glioma therapy which depend on the location of tumor, the grade of malignancy and the cell type. For high grade glioma the treatment usually is a combined therapy, comprising surgery, chemotherapy and radiotherapy [12]. To patients who have glioblastoma presenting with positive neurologic performance status, the present standard treatment includes maximum safe surgical resection with subsequent adjuvant radiotherapy and concurrent temozolomide application [13]. As humanized recombinant monoclonal antibody against vascular endothelial growth factor (VEGF), named Bevacizumab has been approved for the

treatment of recurrent glioblastoma [14, 15].

Though substantial efforts were made in medical technology, the approaches for high grade gliomas are still only palliative [16]. It was suggested to make classification for high grade glioma according to the tumor mass gene expression-profile, and the resulting GBM subtypes were named proneural, neural, classical or mesenchymal [16-18]. It may make the therapy more individualized and efficient for patients according to the GBM genetic classification in the future.

1.2 Pericytes

1.2.1 Definition of pericyte

Pericytes as a new cell type were discovered by Charles Rouget in 1873, and were called Rouget cells in the beginning and renamed pericytes later [19]. Pericytes display a perivascular morphology and usually wrap themselves around blood vessels [20]. Most peripheral pericytes are regarded as arising from the mesoderm, nevertheless others originate from the neural crest, for example brain pericytes [21]. Usually pericytes are located on the surface of capillaries, they interact with endothelial cells which are situated on the same basement membrane [22]. Pericytes have similar features with vascular smooth muscle cells: they are capable of regulating vasomotion and containing contractile filaments consist of alpha- smooth muscle actin (αSMA) and vimentin [19]. The density of pericytes also varies in different area of the body, which is already shown to correlate with the blood pressure levels [23]. It is generally considered that the vasculature of central nervous system (CNS) is covered by most pericytes with a ratio of 1:3-1:1 between pericytes and endothelial cells. Moreover, the coverage is up to approximately 30% on the abluminal surface [24, 25].The highest coverage of pericytes can be detected in the brain and retina which is probably related to the regulation of tight endothelial barrier [26].

1.2.2 Protein and receptor expression on pericytes

Pericytes express a certain range of proteins and receptors, which are considered as

markers for pericytes. The membrane markers include neuron-glial 2 (NG2), CD146, platelet-derived growth factor receptor β (PDGFRβ), endoglin and aminopeptidases A and N (CD13) [27-29]; cytosolic markers include desmin, vimentin and nestin (table 1.2). Routinely these markers are used to identify pericytes, however, they are not expressed by pericytes in every organ or tissue and neither one of them is completely specific. It could be due to the plasticity of pericytes, since different markers can be expressed by pericytes in different organs and tissues at different developing stages [30].

Table 1.2 Cytosolic and membrane-bound markers for the identification of vascular mural cells [19]

Expressed in:	Pericytes	VSMCs	Arterioles	Capillaries	Venules	Remarks
Cytosolic markers						
Alpha-smooth muscle actin (αSMA)	+	+	+	−	+	Most frequently used and best characterized. Also a marker for VSMCs.
Non-muscle myosin	+	−	-	+	+	Present in relatively high concentration in capillary pericytes, absent in VSMCs.
Tropomyosin	Unknown	+	−	+	+	Part of the actin cytoskeleton.
Desmin	+	+	+	+	+	Useful marker in tissues other than skeletal muscle and heart tissue. Expressed on intermediate filament proteins in pericytes that are in direct contact with underlying endothelium. Also expressed by VSMCs.
Vimentin	+	+	+	+	+	Component of intermediate filaments.
Nestin	+	+	+	+	+	An intermediate filament protein that is expressed mostly in nerve cells during early stages of development. In adulthood replaced by tissue specific intermediate filaments in mural cells.
Regulator of G protein signalling 5 (RGS5)	+	+	+	+	+	Tested in PDGFRβ- or PDGF-β deficient mice. Marker for developing pericytes independent of PDGF-β signalling.
Membrane bound markers						
Platelet-derived growth factor receptorβ (PDGFRβ)	+	+	+	+	+	Expressed by developing pericytes and precursor pericytes. Also a tyrosine kinase receptor important for pericyte function.
CD146	+	+	+	+	+	Transmembrane glycoprotein. EC antigen also expressed at the surface of pericytes and in larger blood vessel types.
Aminopeptidases A and N (CD13)	+	+	+	+	+	Type II membrane zinc dependent metalloproteases.
Endoglin (CD105)	Unknown	+	+	+	+	TGF-β1 co-receptor required for angiogenesis. Also a marker for ECs.
Neuron-glial 2 (NG2)	+	+	+	+	−	Broadly expressed in pericyte population, expressed during vascular morphogenesis. Also expressed by larger blood vessel types, and by oligodendrocytes.

1.2.3 Pericyte function

I The role of pericytes in blood-brain-barrier (BBB)

In the central nervous system, pericytes are components of a complex structure called neurovascular unit (NVU) which consists of neurons, endothelial cells, microglial cells and astrocytes [31]. The role of astrocytes has been well described in BBB regulation, and it also has been reported that NVU pericytes were involved. During embryogenesis, recruitment of pericytes is essential for BBB formation, and the coverage of pericytes is considered as a crucial factor for vascular permeability [32]. Bell and colleagues reported vivo evidences that proves the pericyte-involvement in BBB, they suggested that BBB breakdown, the accumulation of macro- molecules and toxic serum proteins were related to the decrease of pericyte coverage [33]. Pericytes are regarded as being capable of controlling blood flow and trans-endothelial transport, therefore pericytes can play an important role in blood-brain barrier formation and its functionality [34].

II Angiogenesis

Pericytes play an essential role in vessel formation, stabilization and remodeling [35]. There are several factors and signaling pathways suggested to play a significant role in intercellular communication between endothelial cells and pericytes, such as platelet-derived growth factor B (PDGF-B), angiopoietins, transforming growth factorβ (TGFβ) and spingosine-1-phosphate [26, 30, 36]. In genetically modified mouse models, the significance for the signaling pathway of PDGF-B/PDGFRb has

been greatly emphasized [37]. PDGF-B is considered to have the high affinity to bind with PDGFRb and PDGFRb is abundant on pericytes. Sprouting endothelial cells can produce PDGF-B during angiogenesis promoting the attachment and recruitment of pericytes [38]. Impaired PDGF-B/PDGFRb signaling can lead to unsuccessful pericyte recruitment and decreased microvascular coverage of pericytes, which finally results in endothelial hyperplasia, formation of microaneurysms and abnormal vascular morphogenesis [39]. Genetic deletion of PDGF-B or PDGFRb can lead to perinatal death because of vascular dysfunction [40, 41]. When investigating the coverage of pericytes in the retina of genetically modified mice, a decreased amount of pericytes has been discovered and leaded to serious hemorrhage [42]. The significance of PDGF-B is highlighted in many studies, which demonstrate that PDGF-B ablation can lead to decreased retinal pericytes coverage resulting in altered capillary diameter, microaneurysms and regressing capillary branches [43]. We can conclude that the well-controlled and balanced secretion of endothelial PDGF-B plays an important role in developing and maintaining the vasculature in CNS.

III Contractile function

In larger vessels VSMCs play an essential role in vasodilatation and vasoconstriction, while in the capillaries pericytes have great effect on regulating vascular diameter. As pericytes are located on the surface of capillaries and express contractile proteins, so the pericytes are suggested to take part in the regulation of microvascular blood flow [44]. Fernández-Klett demonstrated that in vivo pericytes are able to regulate blood

flow in capillaries of the brain cortex [45]. It was suggested that pericytes might be playing a role as pre-capillary sphincters, since the contractile proteins are abundantly located in the transitional position of arterioles and capillaries [46]. The vessel diameter can be influenced by different vasoactive circulatory ligands through activating pericyte cell-surface receptors. For example, endothelin-1, angiotensin 2, histamine and serotonin can produce vasoconstriction, whereas β2-adrenoceptors, cholinergic agonists and nitric oxide can produce vasodilation [47]. These findings are in accord with the theory that the contractility of pericytes contributes to the microvasculature blood flow regulation.

1.3 Aims of the study

Pericytes are considered as a component of the vessel structure and they play an important role in blood-vessel formation and maintenance, but the role of pericyte progenitor cells was not studied previously because they were not discovered. In this study we established a NesCreER^{T2}-Ai9tdTomato double transgenic mouse model that allowed tracing the fate of nestin-expressing cells in high-grade glioma and tumor-free brain over postnatal period, the pericyte progenitor cells were investigated in the current study.

The aim of this study:

(1) To trace cells of the pericyte-lineage throughout glioma angiogenesis in vivo;

(2) To trace cells of the pericyte-lineage throughout postnatal brain development;

(3) To compare the cell populations identified with different nesCreER^{T2}-mouse models;

(4) To trace cells of the pericyte-lineage in the developing vasculature of the retina.

2. Materials

2.1 Technical equipment

Table 2.1 Technical equipment

Lab appliance	Company
Balances-MonoBloc	Mettler Toledo
Balances-AG204	Mettler Toledo
Centrifuge	Thermo Fisher Scientific GmbH
Fridge (-4℃ ,-20 ℃)	LIEBHERR GmbH
Fridge (-80 ℃)	LIEBHERR GmbH
Hera safe hood	Thermo Fisher Scientific GmbH
Incubator	Kendro GmbH
Laboratory Labeling system	LABXPERT TM
Microscope (fluorescence) -Axiovert 25	Carl Zeiss Microscopy GmbH
Microscope (transmitted light) - Axioskop 2	Carl Zeiss Microscopy GmbH
Microscope (confocal) TCS SP5	Leica Microsystems Vertrieb GmbH
Microscope camera- AxioCam MRm	ZEISS GmbH
Microtome Slide 2003	PFM medical AG
Magnetic Hotplate Stirrer	VWR International GmbH
Perfusion system-Dose IT P910	Integra Biosciences AG
Pep-pen	Dako GmbH
Pipette boy	Eppendorf GmbH
Pipettes	Eppendorf GmbH
Shaker	Biozyme Scientific GmbH
12- and 24-well plates	TPP Techno GmbH

2.2 Consumables

Table 2.2 Consumables

Product	Supplier
Tubes (0.5ml,1ml,2ml)	Eppendorf GmbH
Tubes (15ml,50ml)	VWR GmbH
Pipette tips (10µl, 20µl, 200µl ,1000 µl)	Eppendorf GmbH
Slide for immunolabelling	Gerhard Menzel GmbH
cover slips	Gerhard Menzel GmbH
Plate (12 wells,24 wells)	TPP GmbH
Tissue-Tek Cryomold (15mm×15mm×15mm)	Sakura Finetek USA

2.3 Reagents and Chemicals

Table 2.3 Reagents and Chemicals

Product	Supplier
Acetone100%	Sigma GmbH
Antibody diluent	Dako
CIdu-C6891(5-Chloro-2'-deoxyuridine)	Sigma GmbH
Corn oil	Sigma GmbH
DAPI	Sigma GmbH
DAB-DC135c006	DCS Labline
DAB-substrate-PC136R100	DCS Labline
Donkey serum	Sigma GmbH
Dual Endogenous Enzyme block	Dako
Ethanol-70%	CLN GmbH Chemikalien Laborbedarf

Ethanol-96%	CLN GmbH Chemikalien Laborbedarf
Ethanol-100%	CLN GmbH Chemikalien Laborbedarf
Eosin G-solution	Sigma GmbH
Ethylene	Sigma GmbH
Cryomatrix	Thermo Sientific
Glycerol	Sigma GmbH
Goat serum	Sigma GmbH
Hope	DCS Labline
Hemalaun	Carl Roth GmbH
Idu-17125 (5-iodo-2'-deoxyuridine)	Sigma GmbH
ketamine	Zoetis Deutschland GmbH
0.9%Nacl	B.Braun Melsungen AG
2%Rompun	Bayer Vital GmbH
Mounting Medium	IBIDI GmbH
PBS	Apotheke Klinikum der Universität München
Paraformaldehyde (PFA)	Sigma GmbH
Protein Block	Dako GmbH
Sucrose	Sigma GmbH
Tamoxifen-T5648	Sigma GmbH
Triton X-100	Roche Diagnostics GmbH
Tween-20	Sigma GmbH
Xylol	Sigma GmbH
X-gal	Thermo Fisher

2.4 Immunohistochemistry

2.4.1 Primary Antibodies

Table 2.4.1 Primary Antibodies

Immunogen	Host Species	Isotype	Catalog number	Dilution	Provider
NG2	Rabbit	IgG	ab5320	1:200	Millipore AG
Desmin	Rabbit	IgG	ab15200	1:200	Abcam,
SOX2	Rabbit	IgG	Ab97959	1:200	Abcam
PDGFRß	Goat	lgG	AF1042	1:200	R+D GmbH
CD146	Rabbit	IgG	Ab75769	1:800	Abcam
CNpase	mouse	IgG	Ab6319	1:250	Abcam
RFP	Rabbit	IgG	ab62341	1:200	Abcam,
Iba1	Rabbit	IgG	019-19741	1:500	Wako GmbH
GFAP	Rabbit	IgG	Z0334	1:500	Dako
CD31	Rat	IgG	550274	1:50	Cat
CD45	Rat	IgG	110-93609	1:100	Novus-USA
VWF	Rabbit	IgG	A0082	1:400	Dako GmbH
IB4-biotinylated			B-1205	1:100	Vector
IB4-FITC			L-2895	1:200	Sigma
β-gal	Rabbit	IgG	A11132	1:300	Molecular Probes
SMA	Rabbit	IgG	ab66133	1:400	Abcam
S-100ß	mouse	IgG	S2532	1:500	Sigma

2.4.2 Secondary antibodies

Table 2.4.2 Secondary Antibodies

Antigen	Host Species	Conjugation	Catalog number	Dilution	Provider
Rabbit IgG	Donkey	Alexa Fluor 488	711545152	1:500	Jackson Immuno-Research, West Grove, PA, USA
Rabbit IgG	Donkey	Alexa Fluor 594	711585152	1:500	Jackson Immuno-Research, West Grove, PA, USA
Rabbit IgG	Donkey	Cy3	71116152	1:500	Jackson Immuno-Research, West Grove, PA, USA
Rabbit IgG	Donkey	biotinylated	711065152	1:250	Jackson Immuno-Research, West Grove, PA, USA
Goat IgG	Donkey	biotinylated	705065147	1:250	Jackson Immuno-Research, West Grove, PA, USA
Goat IgG	Donkey	Alexa Fluor 488	705545147	1:500	Jackson Immuno-Research, West Grove, PA, USA
Goat IgG	Donkey	Cy3	705165147	1:500	Jackson Immuno-Research, West Grove, PA, USA
Rat IgG	Donkey	biotinylated	712065153	1:250	Jackson Immuno-Research, West Grove, PA, USA

Mouse IgG	Donkey	Cy5	715175150	1:500	Jackson Immuno-Research, West Grove, PA, USA
Chicken IgG	Donkey	biotinylated	703065155	1:250	Jackson Immuno-Research, West Grove, PA, USA

2.4.3 Streptavidin-conjugated fluorophores

Table 2.4.3 Streptavidin-conjugated fluorophores

Fluorescence	**Catalog Number**	**Dilution**	**Provider**
Alexa Fluor 488	016540084	1:500	Jackson Immuno-Research, West Grove, PA, USA
Alexa Fluor 594	016580084	1:500	Jackson Immuno-Research, West Grove, PA, USA
Alexa Fluor 647	016600084	1:500	Jackson Immuno-Research, West Grove, PA, USA
Streptavidin-HRP	SA-5004	1:200	Vector

2.5 Software

Table 2.5 Software

Software	Provider
Microsoft office 2007	Microsoft
GraphPad Prism 6	Graph Pad Software
Image J	National Institutes of Health, USA
Adobe Illustrator CS6	Adobe Systems
Adobe Photoshop CS6	Adobe Systems
Windows 7 system	Microsoft

3. Methods

3.1 Mouse models

In this study we used NesCreER^{T2} and Ai9tdTomato double transgenic mouse models. As an essential tool for the generation of conditional mouse mutations, the Cre/loxp recombination system is used for the induction of a permanent reporter achieved by the red fluorescent protein td-Tomato. Cre can recombine the gene sequence between two 34-bp DNA recognition sites which are called loxP sites. The animals used in this study express Cre recombinase under the control of the nestin promoter [48]. The nestin gene is active in neural stem cells and also other progenitor cells during the development of the central nervous system (CNS) [49]. CreER, a fusion protein of Cre and the human estrogen receptor, is tamoxifen inducible. Without tamoxifen CreER will stay in cytoplasm and has no function, but it becomes activated by tamoxifen administration. After being activated, the CreER will be translocated into the nucleus and recombine the gene sequence of loxP-flanked sites [50]. The reaction of CreER^{T2} with tamoxifen is more efficient than Cre-ER^{T} [51], thus, the mice with the expression of CreER^{T2} under the control of nestin promoter can provide a helpful tool for investigating progenitor cells in physiology and pathology of the brain. When NesCreER^{T2} mice and Ai9-tdTomato mice are crossed generating NesCreER^{T2} x Ai9tdTomato mice, tamoxifen administration will activate Cre recombinase and can excise a floxed stop cassette and will disinhibit the expression of RFP. As a result, RFP as a reporter molecule can be used as a fate-mapping tool for nestin- expressing cells in NesCreER^{T2} x Ai9tdTomato mice.

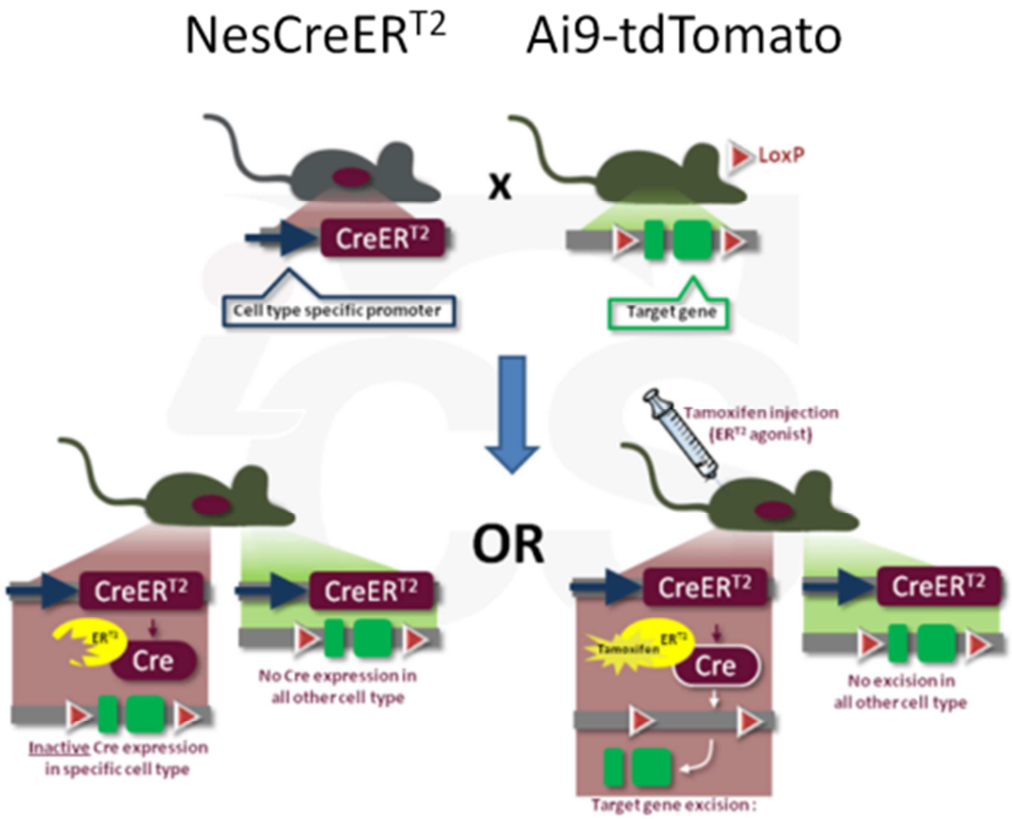

Fig. 3.1 The NesCreERT2-Ai9tdTomato mouse model

(Modified from http://www.ics-mci.fr)

For all mouse treatments, we followed the rules and regulations of the Regierung Von Oberbayern according to the animal protection act. All the mouse experiments were performed in the Walter Brendel Centre of the Klinikum Groβhadern LMU.

In this study, the NesCreER^{T2} x Ai9tdTomato transgenic mice were used. There were 3 experiment mouse groups, all mice carried both the NesCreER^{T2} and the Ai9tdTomato transgene. the mice in each group were inoculated 1X10^{5} GL261(1ul) glioma cells on day 0 and administrated with tamoxifen on day 4-6, the tumor growth

was observed over a time course (7 days,14 days and 21 days).

As controls, there were 3 further mouse groups: negative control group 1, negative control group 2 and positive control group 3. The mice in each group were inoculated $1X10^5$ GL261 (1ul) glioma cells on day 0 and sacrificed at day 14, they were genetically modified as following:

Negative control group 1: nes-CreER^{T2} (–); Ai9-tdTomato (+); TAM i.p. on 4-6d;

Negative control group 2: nes-CreER^{T2} (+); Ai9-tdTomato (+); TAM i.p. (–);

Positive Control group 3: nes-CreER^{T2} (+); Ai9-tdTomato (+); TAM i.p. on 4-6d;

To further investigate the lineage of nestin positive cells in the NesCreERT2-tdTomato mouse strain, gene recombination was induced after birth (at postnatal day 0; po), and the mice were sacrificed after 3 weeks (p21).

Furthermore, another mouse model named Jnes-CreER^{T2} were also used in this study (the transgenic nestin-promoter element in Jnes-CreER^{T2} is different from the Nes-CreER^{T2}). the mice were inoculated $1X10^5$ GL261(1ul) glioma cells on day 0 and administrated with tamoxifen on day 4-6, the tumor growth was observed over a time course (14 days and 21 days).

3.1.1 Tumor cells inoculation

1. Anesthesia

Preparation of narcotic

10% Ketamine	1.02ml
2% Rompun	0.36ml
0.9% Nacl	4.86ml

Mice received the narcotic according to body weight (7µl/g) by intra-peritoneal injection (i.p), and the eyes were protected with Bepanthen.

2. Tumor cells inoculation.

After anesthesia, mice were fixed on the stereotactic frame in a flat-skull position, then disinfection was performed with 10% potassium iodide solution, the skin of the skull was incised carefully with the scalpel. The accurate inoculation position (1,5mm anterior of the bregma; 1.5mm right of the bregma) was confirmed by Vernier Caliper, the skull point was drilled carefully by a 21-gauge needle tip. $1X10^5$ GL261 (1 ul) glioma cells were injected at a depth of 3mm from the skull surface. Then the syringe-needle was retreated slowly about 1 mm/1 min. After the needle was completely retreated out, the incision was carefully sutured.

3.1.2 Tamoxifen administration

Preparation of tamoxifen

Tamoxifen (T5648,Sigma) 20mg	Corn oil (C8267,Sigma) 1ml

Mice were given tamoxifen according to body weight (75mg/kg) by intra-peritoneal injection (i.p) every 24 hours for 3 days.

3.1.3 CIdu and Idu administration

Preparation of CIdu and Idu

5-Chloro-2'-deoxyuridine (CIdu) 8.55mg	0.9% NaCl 1ml
5-iodo-2'-deoxyuridine (Idu) 11.35mg	PBS (0.1M)+5N NaOH 2 drops/10 ml PBS, 1ml

Mice were given CIdu 48 hours before sacrifice according to body weight (42.75mg/kg) by intraperitoneal injection (i.p); and Idu (56.75mg/kg) 5 hours before sacrifice also by i.p.

3.1.4 Sacrifice and perfusion of mice

First mice were injected with a narcotic according to body weight (7µl/g) by intraperitoneal injection (i.p), and then perfused by perfusion system (8.7mL/min) through the heart with 20ml PBS and 4%PFA 10ml.

3.1.5 Fixation and tissue harvest

Brains were immersed in 4%PFA for 48 hours at +4°C, followed by incubation in 30% sucrose for 48 hours at +4°C; brains were embedded in Cryomatrix (ThermoSientific) and frozen. Tissue was cut into 40µm sections with a microtome, and stored in 24-well plates filled with cryoprotectant (Glycerol 125ml+Ethylene glycol 125ml+Phosphate buffer 250ml) at -20°C.

3.2 Immunohistochemistry (IHC)

Immunohistochemistry technology is widely used to label Specific molecular markers, it depends on the principle that an antibody can specifically bind to antigens. In this study, we mainly perform Immunofluorescence staining.

3.2.1 Immunofluorescence staining for free-floating sections

Part 1: without biotinylated- Streptavidin Conjugation

The free-floating sections were usually applied in 24-well plates filled with cryoprotectant at -20°C. First we transferred 3-5 sections to a new 12-well plates with PBT (PBS+0.1%TWEEN-20), and washed the sections for 3 times for 5 minutes on an orbital shaker; And next the sections were incubated with Dual Endogenous Enzyme block (S2003, Dako) for 20 minutes (room temperature) to block the

endogenous peroxidase; After that the sections were washed 3 times with PBT and then incubated with protein block (X0909, Dako) for 1hour (room temperature); After then the sections were incubated with primary antibody diluted in Antibody diluent (S3022, Dako) overnight at +4°C; The next day, the sections were washed 3 times with PBT and subsequently incubated with secondary antibody diluted in Antibody diluent (S3022, Dako) for 2 hours (room temperature); Afterwards the sections were washed 3 times with PBT again and incubated with Alexa-Hoechst (dillution1:1000) for 1 minute (room temperature); At last, the sections were carefully mounted on the slide and covered with fluorescence mounting medium.

Part 2: with biotinylated- Streptavidin Conjugation

First the sections were transferred to a new 12-well plates with PBT (PBS+0.1%TWEEN-20) and washed for 3 times for 5 minutes on an orbital shaker; And next the sections were incubated with Dual Endogenous Enzyme block (S2003, Dako) for 20 minutes (room temperature) to block the endogenous peroxidase; After that the sections were washed 3 times with PBT and then incubated with protein block (X0909, Dako) for 1hour (room temperature); After then the sections were incubated with primary antibody diluted in Antibody diluent (S3022, Dako) overnight at +4°C; The next day, the sections were washed 3 times with PBT and subsequently incubated with secondary antibody with biotinylated Conjugation diluted in Antibody diluent (S3022, Dako) for 3 hours (room temperature); Afterwards the sections were washed 3 times with PBT again and incubated with Alexa Fluor 488/594/674 with

Streptavidin Conjugation diluted in Antibody diluent (S3022, Dako) for 2 hours (room temperature); And then the sections were washed 3 times with PBT again and incubated with Alexa-Hoechst (dillution1:1000) for 1 minute (room temperature); At last, the sections were carefully mounted on the slide and covered with fluorescence mounting medium.

3.3 Quantification and analysis

To evaluate the staining, microscopes (include fluorescence microscope and confocal microscope) were applied.

Fluorescence microscopy

For the immunofluorescence staining, a fluorescence microscopy (with the wavelength range 340-700nm) was used.

Confocal Microscopy

Confocal microscopy was also called confocal laser scanning microscopy (CLSM), it is able to collect image sets from different depths of the thick sections, from which it can reconstruct the three-dimensional structures. It is widely used to analyze the co-localization by setting different channel parameter.

All the quantifications were performed using a 20X magnification adjective. For the brain sections with tumor, usually 3 areas within tumor were randomly selected; 2 areas both in peritumoral area and contralateral tumor free area were randomly selected. For the tumor free sections, 4 areas were randomly selected from both cortex

sides, brain stem and the area near sub-ventricular zone. Each quantification was performed manually according to the pictures under the applying of ImageJ software. The software of GraphPad Prism 6 was used for the statistical analysis including unpaired t-tests.

4. Results

4.1 RFP expression in the NesCreER^{T2}-tdTomato mouse model

In this study we used the NesCreER^{T2} x Ai9tdTomato mouse model expressing RFP as a fate-mapping marker for nestin positive cells. In order to investigate the expression of RFP in the mouse brain, cells which are RFP positive were quantified on brain sections of glioma-inoculated and tumor-free mice.

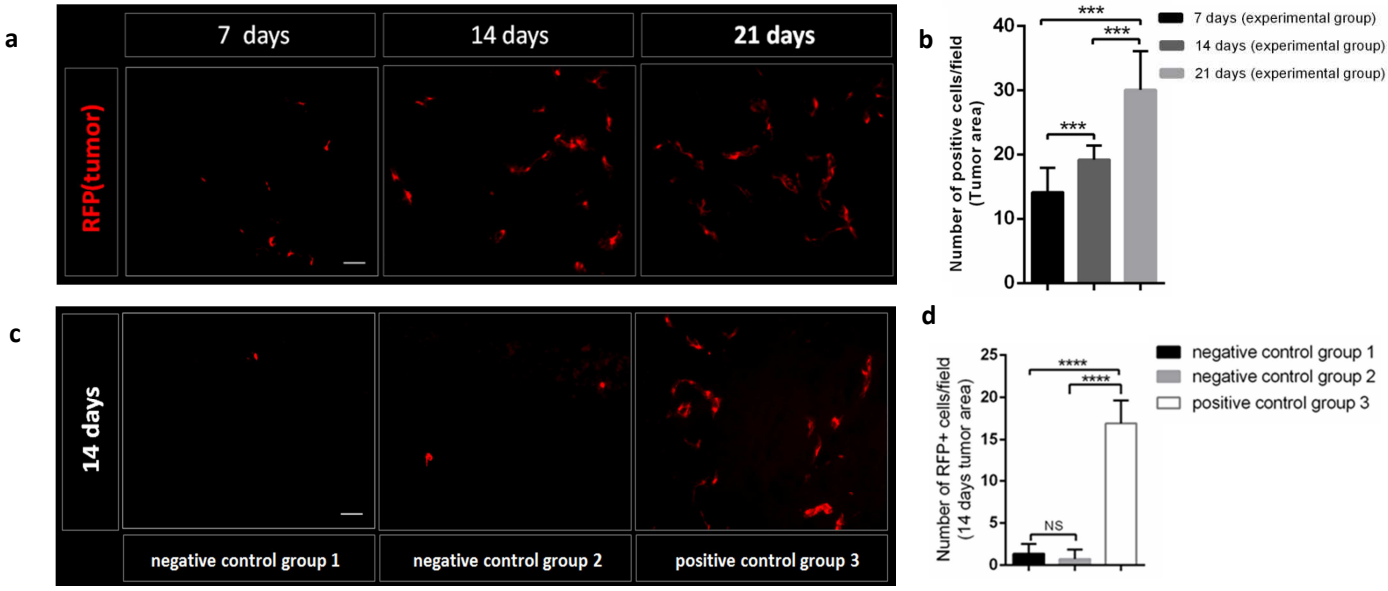

Figure 4.1 RFP expression in the NesCreER^{T2} x Ai9-tdTomato mouse model.

a. RFP positive cells were observed in the tumor area over a time course (7 days, 14 days and 21 days); **b.** Quantification of RFP positive cells in the tumor area: The number of RFP positive cells increases significantly from 7 days to 14 days and 21 days ($p < 0,01$ for all groups); **c.** RFP positive cells were observed in the tumor area in a control group (growth time: 14 days); **d.** Quantification of RFP positive cells in the tumor area: The number of RFP positive cells in negative control groups was significantly lower as compared to the experimental group ($p< 0,001$), but the number of RFP positive cells between the two negative control groups showed no difference. Scale bars in **a,c,** 100 µm.

There were 3 experiment mouse groups, the mice in each group were inoculated $1X10^5$ GL261(1ul) glioma cells on day 0 and administrated with tamoxifen on day 4-6, the tumor growth was observed over a time course (7 days,14 days and 21 days). The number of RFP positive cells in the tumor area increases significantly from 7 days to 14 days and 21 days (Figure 4.1B, $p < 0.01$). After 21 days, the vast majority of RFP positive cells consistently appear perivascular-like. Besides the tumor area, RFP positive cells were also observed in peritumoral areas and the contralateral hemisphere, but here the number of RFP positive cells was much lower than in the tumor area (not shown). Hence, the traced cells of the nestin positive lineage are mainly located in the tumor area.

There were 3 groups of experimental control: Negative control group 1, negative control group 2 and positive control group 3 (Figure 4.1C). Few RFP positive cells could be observed in the negative control groups (control group 1, 2) in the tumor area, while a large number of RFP positive cells are visible in the positive control group 3. This indicates that the nes-CreER^{T2} tdTomato mouse model used in the present study allows specific cell tracing and has very little endogenous leakiness (the Cre-independent RFP expression or the entry of tamoxifen-independent Cre recombinase to the nucleus).

4.2 Immunohistochemical characterization of the NesCreER^{T2}-tdTomato mouse model

The morphology and location of RFP-expressing cells indicated that there is genesis of pericytes from the nestin positive linage. The brain tissue was stained with pericyte markers such as NG2, CD146, PDGFRß or desmin, and the analysis of co-localization of RFP positive cells with the pericyte markers was performed by confocal microscopy.

4.2.1 Immunostaining for NG2

Neuron-glial 2 (NG2) was abundantly expressed by pericytes during the stage of vascular morphogenesis [52, 53]. Not only pericytes but also the GL261 glioma cells express NG2 resulting in an extensive intratumoral staining. To test NG2 expression in RFP positive cells over the time course of tumor development, mouse brain samples from different groups (7 days, 14 days, 21 days) were immunostained and analyzed (Figure 4.2.1 a). Confocal picture analysis showed that NG2 staining co-localized with RFP positive cells (Figure 4.2.1b). The number of RFP positive cells and RFP&NG2 double positive cells was also quantified. The date revealed that during tumor progression from 7 days to 14 days and to 21 days, the number of RFP positive cells and RFP&NG2 double positive cells increased (Figure 4.2.1c). After 7 days of tumor progression, few RFP-expressing cells co-localized with NG2, whereas after 21 days of tumor growth most of the recombined cells co-localized with NG2, which indicated that the pericyte progenitor cells (RFP positive and NG2 negative) differentiate into pericytes (RFP positive and NG2 positive) during glioma expansion. Compared to the total amount of RFP expressing cells in the tumor, the percentage of

RFP&NG2 double positive cells significantly increased from 7.58% (7 days) to 18.61% (14 days) and 74.12% (21 days). This indicates that the traced cells from the nestin positive lineage develop into pericytes during glioma expansion (Figure 4.2.1d, e). The longer the time of tumor growth, the more RFP positive cells expressing pericyte markers were detected. Very few RFP&NG2 double positive cells were observed in peritumoral areas and the contralateral hemisphere (Figure 4.2.1 f, g), which indicates that new pericytes derive from pericyte progenitors of the adult brain most prominently during neo-angiogenesis.

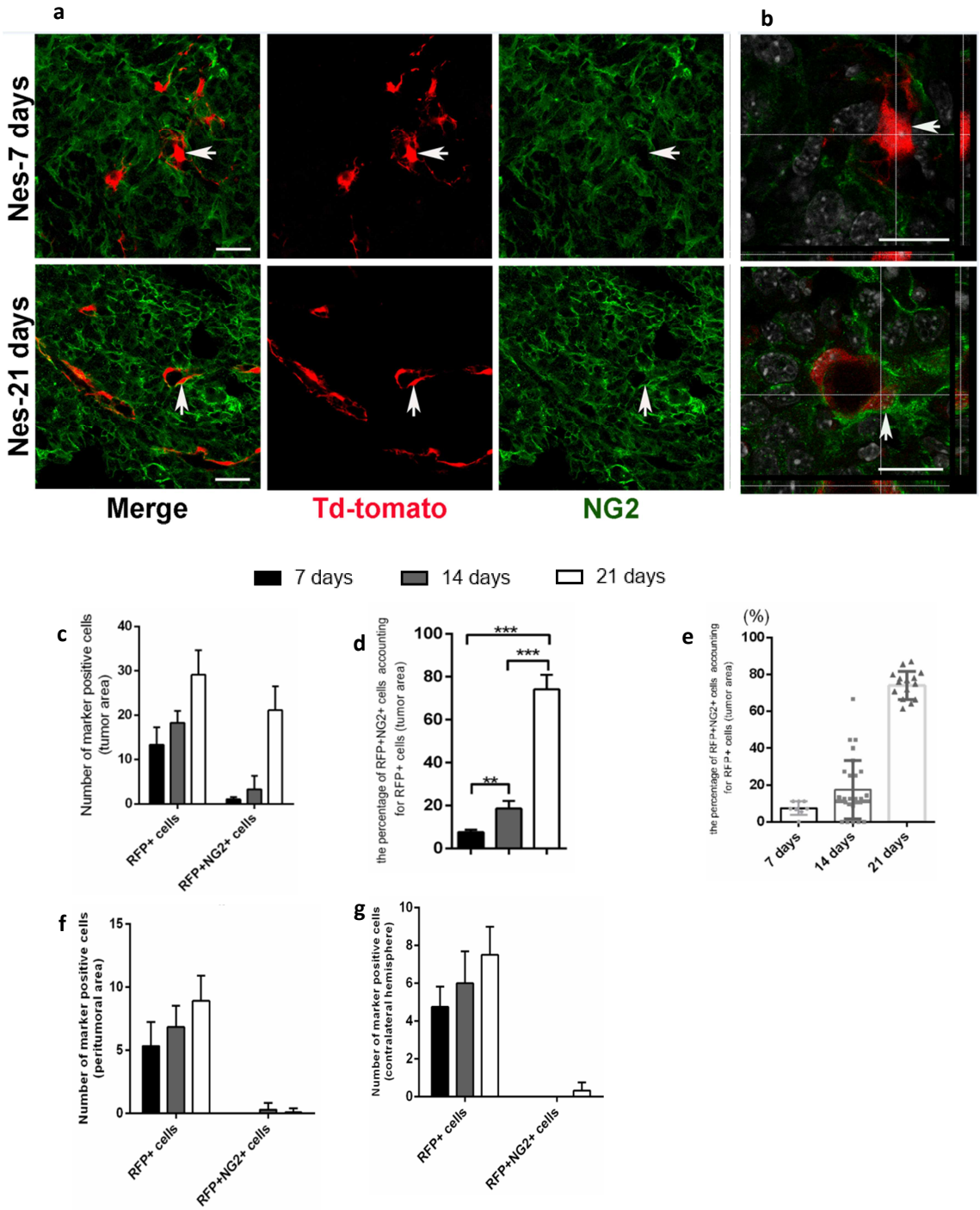

Figure 4.2.1 NG2 expression in the NesCreERT2 TdTomato mouse model.
a. RFP (shown in red) and NG2 (shown in green) expression in the tumor area of the NesCreER^{T2}-tdTomato glioma mouse model is shown at different time points of tumor expansion (7 days and 21 days, 14 days not shown); **b**. Confocal microscopy indicated that NG2 co-localized with RFP-expressing cells: after 7 days, there were very few RFP positive cells co-localized with NG2, but after 21 days, most RFP positive cells co-localized with NG2, which indicated that the pericyte progenitor cells (RFP positive and NG2 negative) differentiate into pericytes (RFP positive and NG2 positive) during glioma expansion; **c.** RFP positive cells and RFP&NG2 double positive cells in tumor area were quantified; **d, e**. The percentage of RFP&NG2 double positive cells accounting for the total RFP positive cells was calculated ($p<0.01$); **f, g**. RFP positive cells and RFP&NG2 double positive cells in peritumoral areas and contralateral hemisphere were quantified. Scale bars in **a,b,** 50 μm.

4.2.2 Immunostaining for CD146

Cluster of differentiation marker 146 (CD146) is a transmembrane glycoprotein and constitutes another membrane bound marker for pericytes [52]. Similar to the NG2 analysis (see above), mouse brain samples from different groups (7 days,14 days,21 days) were stained and analyzed (Figure 4.2.2 a). Confocal pictures showed that CD146 staining also co-localized with RFP positive cells after 21 days (Figure 4.2.2b). RFP positive cells and RFP&CD146 double positive cells were also quantified. The number of RFP positive cells significantly increased from 7 days to 21 days, after 7 days, there were very few RFP positive cells co-localized with CD146, but after 21 days, most RFP positive cells co-localized with CD146, the percentage of RFP&CD146 double positive cells accounting for RFP-expressing cells significantly increased from 19.62% (7 days) to 53.88% (14 days) and 83.46% (21 days). (Figure 4.2.2 d, e), which indicated that the pericyte progenitor cells (RFP positive and CD146 negative) differentiate into pericytes (RFP positive and CD146 positive) during glioma expansion. Also, in the peritumoral areas and contralateral hemisphere, very few RFP&CD146 double positive cells were observed (Figure 4.2.2 f, g). The percentages of RFP&CD146 double positive cells accounting for RFP-expressing cells at 7 days, 14 days and 21 days are similar to the percentages of RFP&NG2 double positive cells: after 7 days, there were very few RFP positive cells co-localized with CD146 or NG2, but after 21 days, most RFP positive cells co-localized with CD146 and NG2, two different markers display a similar role, which confirmed again that the traced cells from nestin positive lineage indeed develop into pericytes over time.

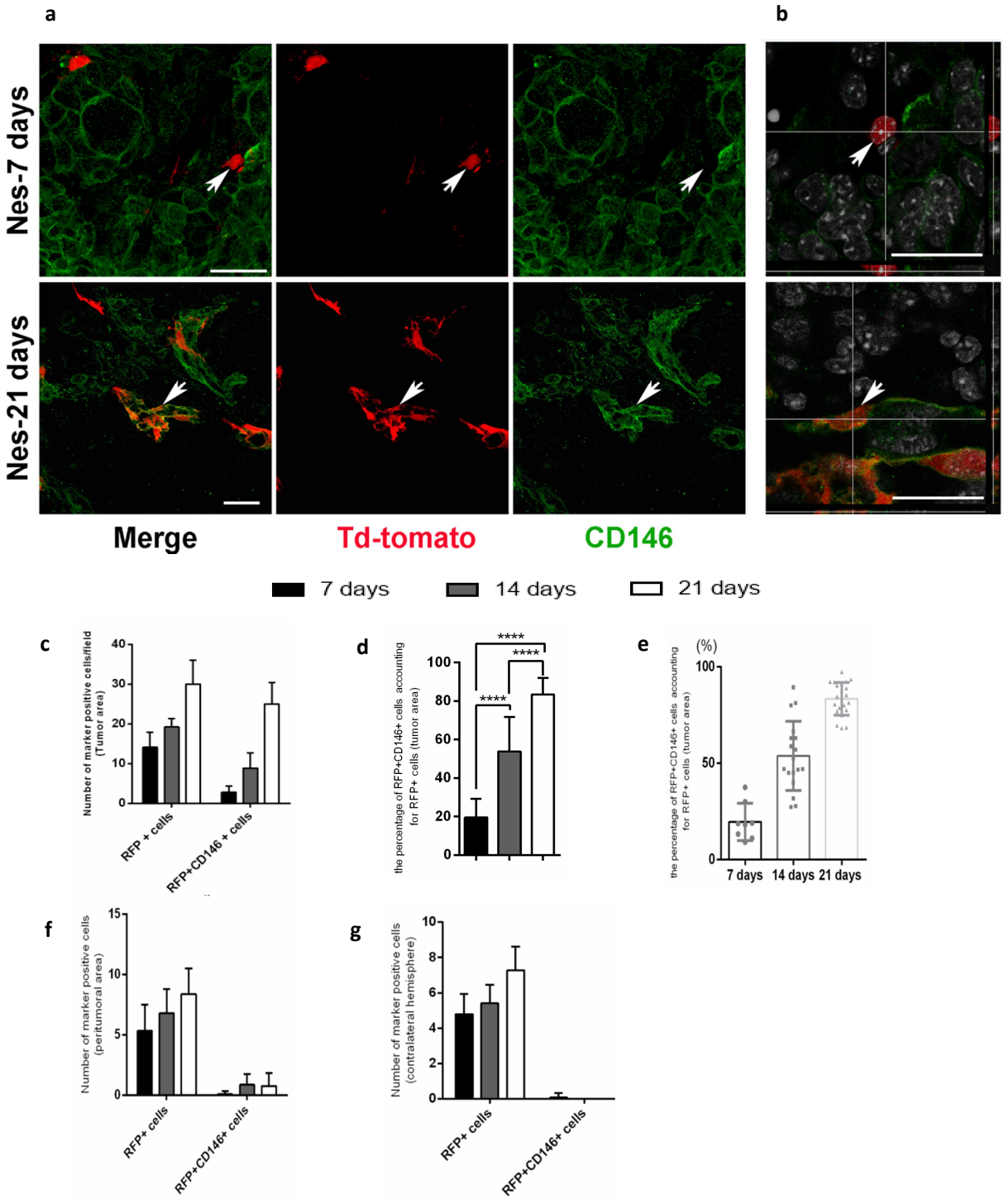

Figure 4.2.2 CD146 expression in the NesCreER^{T2} x Ai9-tdTomato mouse model.

a. RFP (shown in red) and CD146 (shown in green) expression in tumor area of mouse brain samples from different groups (7 days and 21 days, 14 days not shown); **b.** Pictures from confocal microscopy indicated that after 21 days CD146 co-localized with RFP-expressing cells; **c.** RFP positive cells and RFP&CD146 double positive cells in tumor area were quantified from different groups; **d, e**. The percentage of RFP&CD146 double positive cells accounting for the total number of RFP positive cells ($p<0.001$), after 7 days, there were very few RFP positive cells co-localized with CD146, but after 21 days, most RFP positive cells co-localized with CD146, which indicated that the pericyte progenitor cells (RFP positive and CD146 negative) differentiate into pericytes (RFP positive and CD146 positive) during glioma expansion; **f, g.** RFP positive cells and RFP&CD146 double positive cells in peritumoral areas and contralateral hemisphere were quantified from different groups. Scale bars in **a,b,** 50 μm.

4.2.3 Combined immunohistochemical staining for PDGFRß, NG2 and desmin

As shown before, an increasing number of RFP positive cells express markers for pericytes during the time course of tumor development, but it was unclear whether the traced cells express different markers at the same time. To test this, mouse brain samples from the short-term group (7 days) and the long-term group (21 days) were stained and analyzed. Combinatorial staining for PDGFRß&NG2 or PDGFRß&desmin was performed. Confocal image analysis showed that throughout the time course of tumorigenesis increasing numbers of PDGFRß&NG2 or PDGFRß&desmin immunopositive cells co-localized with RFP positive cells (Figure 4.2.3a, b). The number of RFP positive cells and immunopositive cells co-localizing with RFP were quantified. RFP&PDGFRß&NG2 or RFP&PDGFRß&desmin triple positive cells both significantly increased from 7 days to 21 days, and the percentage of triple positive cells accounting for the total amount of RFP-expressing cells in each group was similar (Figure 4.2.3c, d, j, h). After 21 days most of the RFP-expressing cells co-localized with two pericyte markers. However, after 7 days of tumor development only few RFP positive cells were immunostained for both pericyte markers. In the peritumoral area and the contralateral hemisphere almost no RFP& PDGFRß&NG2 or RFP&PDGFRß&desmin triple positive cells were observed (Figure 3.2.3e,f,I,j).

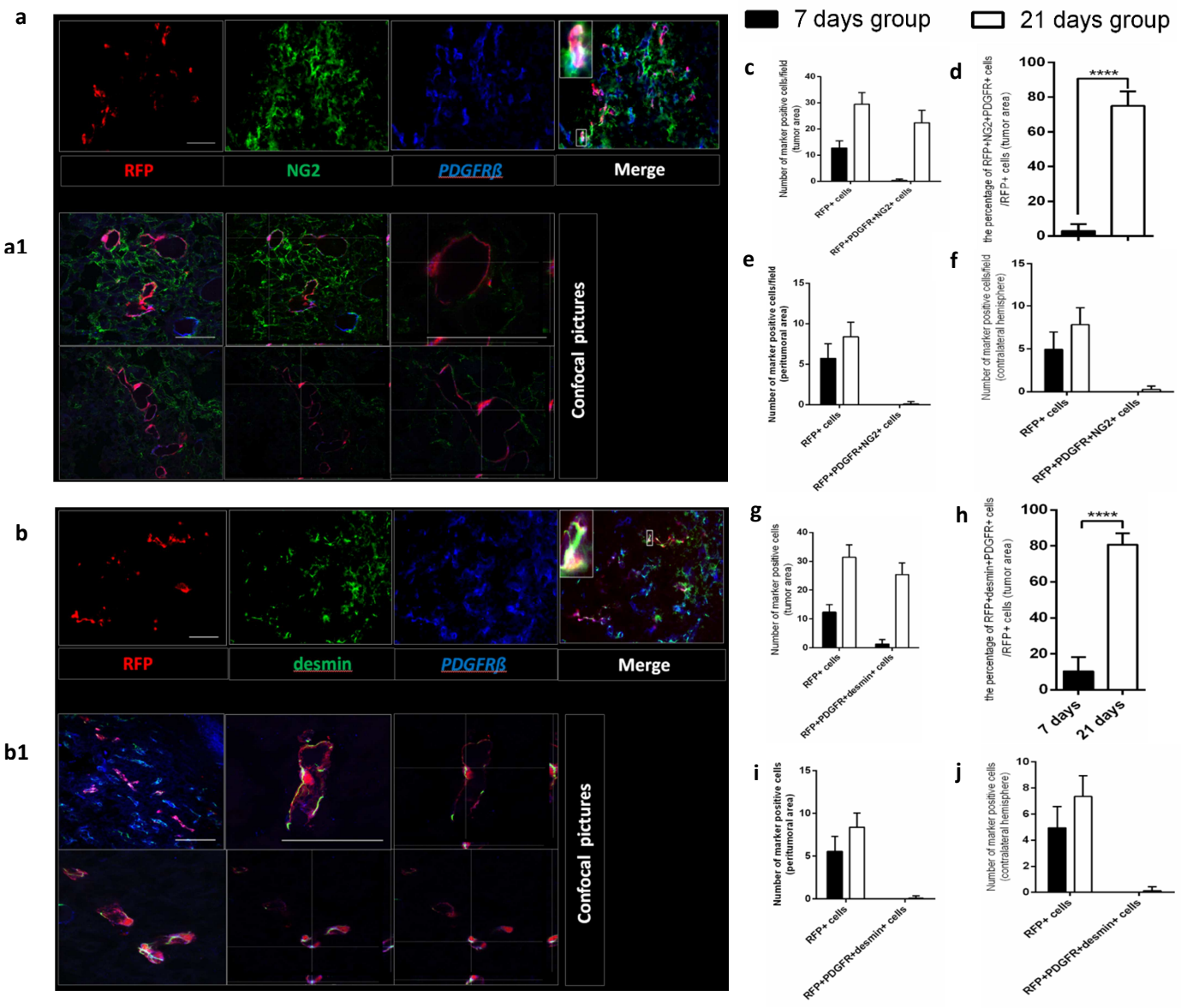

Figure 4.2.3 Combined staining for PDGFRß, NG2 and desmin in the NesCreER^{T2} x Ai9-tdTomato mouse model.

a-b. RFP (shown in red), NG2 or desmin (shown in green) and PDGFRß (shown in blue) expression in tumor area of mouse brain samples from 21 days group; confocal pictures indicated that immunostaining for PDGFRß&NG2/desmin co-localized with RFP; **c, g:** RFP positive cells, RFP&PDGFRß&NG2 or RFP&PDGFRß&desmin triple positive cells in the tumor area were quantified from 7 days group and 21 days group; **d, h:** The percentage of RFP&PDGFRß&NG2 or RFP&PDGFRß&desmin triple positive cells accounting for the total number of RFP positive cells ($p<0.001$); **e,f,i,j:** The number of RFP positive cells and RFP&PDGFRß&NG2 or RFP&PDGFRß&desmin triple positive cells in the peritumoral area and the contralateral hemisphere were quantified. Scale bars in **a,b,** 200µm, **a1,b1,** 100µm.

4.3 Comparative immunohistochemical characterization of the NesCreER^{T2}-tdTomato and JnesCreER^{T2}-tdTomato mouse models

In our study another mouse model named Jnes-CreER^{T2} Tdtomato was used except the Nes-CreER^{T2} Tdtomato mouse model. Many groups have created transgenic mouse models by combining nestin promoter of different spatial specificity with CreER^{T2} that allowing the temporal control of their activity [54]. The potential differences in efficiency and specificity between Nestin-CreER^{T2} and Jnes-CreER^{T2} lines occurred for the combination of design. We can trace the sequence of CreER^{T2} to the same research performed by Chambon and colleagues in both lines [50], but the construct of the nestin promoter in each line is significantly different [55]. To investigate the difference of the fate for traced cells between the Nes-CreER^{T2} and the Jnes-CreER^{T2} mouse models, a series of immunostainings were performed for the JnesCreER^{T2}-tdTomato mouse samples.

4.3.1 RFP expression in the NesCreER^{T2}-tdTomato and JnesCreER^{T2}-tdTomato mouse models

As explained above, RFP was used as a fate-mapping marker for nestin positive cells. In order to compare the expression of RFP in the tumor area of both transgenic mouse strains (NesCreER^{T2} or JnesCreER^{T2}), the RFP positive cells were quantified in samples obtained after 14 days or 21 days of glioma genesis.

The number of RFP positive cells in the tumor area also increases significantly from 14 days to 21 days in the JnesCreER^{T2} transgenic mouse strain, but at both time points (14 days or 21 days) the number of RFP positive cells was much lower in the JnesCreER^{T2} mouse strain as compared to the NesCreER^{T2} mouse line (the differences at both time points are highly significant).

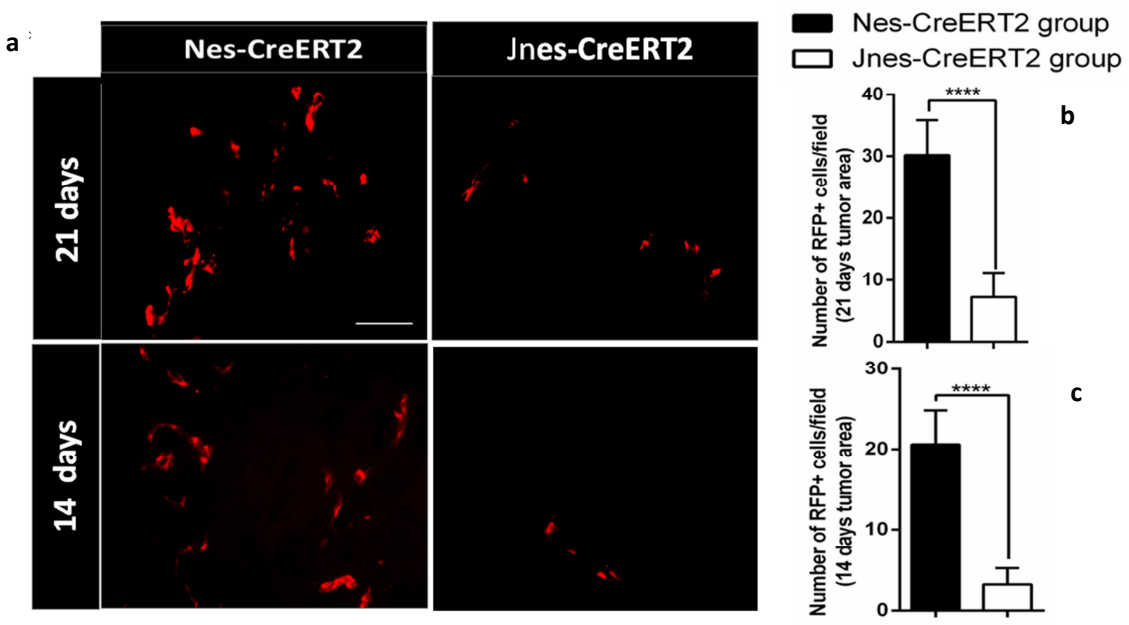

Figure 4.3.1 RFP expression in the NesCreER^{T2}-tdTomato and JnesCreER^{T2}-tdTomato mouse models

a. RFP positive cells (shown in red) in the tumor area from NesCreER^{T2} and JnesCreER^{T2} mouse strains in 14 days and 21 days; **b, c.** Quantification of RFP positive cells in the tumor area from NesCreER^{T2} and JnesCreER^{T2} groups , at both time points the number of RFP positive cells in the JnesCreER^{T2} mouse strain was much lower as compared to the NesCreER^{T2} mouse strain ($p<0.001$). Scale bars in **a,** 200μm.

4.3.2 Investigation for the fate of RFP positive cells in the JnesCreER^{T2}-tdTomato mouse model.

In NesCreER^{T2}-tdTomato mice, most of the traced cells (RFP positive cells) expressed pericytes markers (such as NG2, PDGFRß, desmin or CD146) after 21 days of tumor growth (see Fig.4.2.1- 4.2.3), but in the JnesCreER^{T2}-tdTomato mouse model the co-localization with pericyte markers remained to be determined. To observe this, immunostainings for pericyte markers NG2 and PDGFRß were performed for the JnesCreER^{T2} mouse samples (Figure 4.3.2 a,b). RFP positive cells, RFP&NG2 double positive cells and RFP&PDGFRß double positive cells were quantified (Figure 4.3.2 c-d), there was no pericyte marker co-localized with RFP positive cells in mice of the JnesCreER^{T2} strain. These data show that only the NnesCreER^{T2}-tdTomato mouse strain is a lineage tracing model for pericytes, while the JnesCreER^{T2}-tdTomato mouse line is not indicating cells acquiring a pericyte cell-fate.

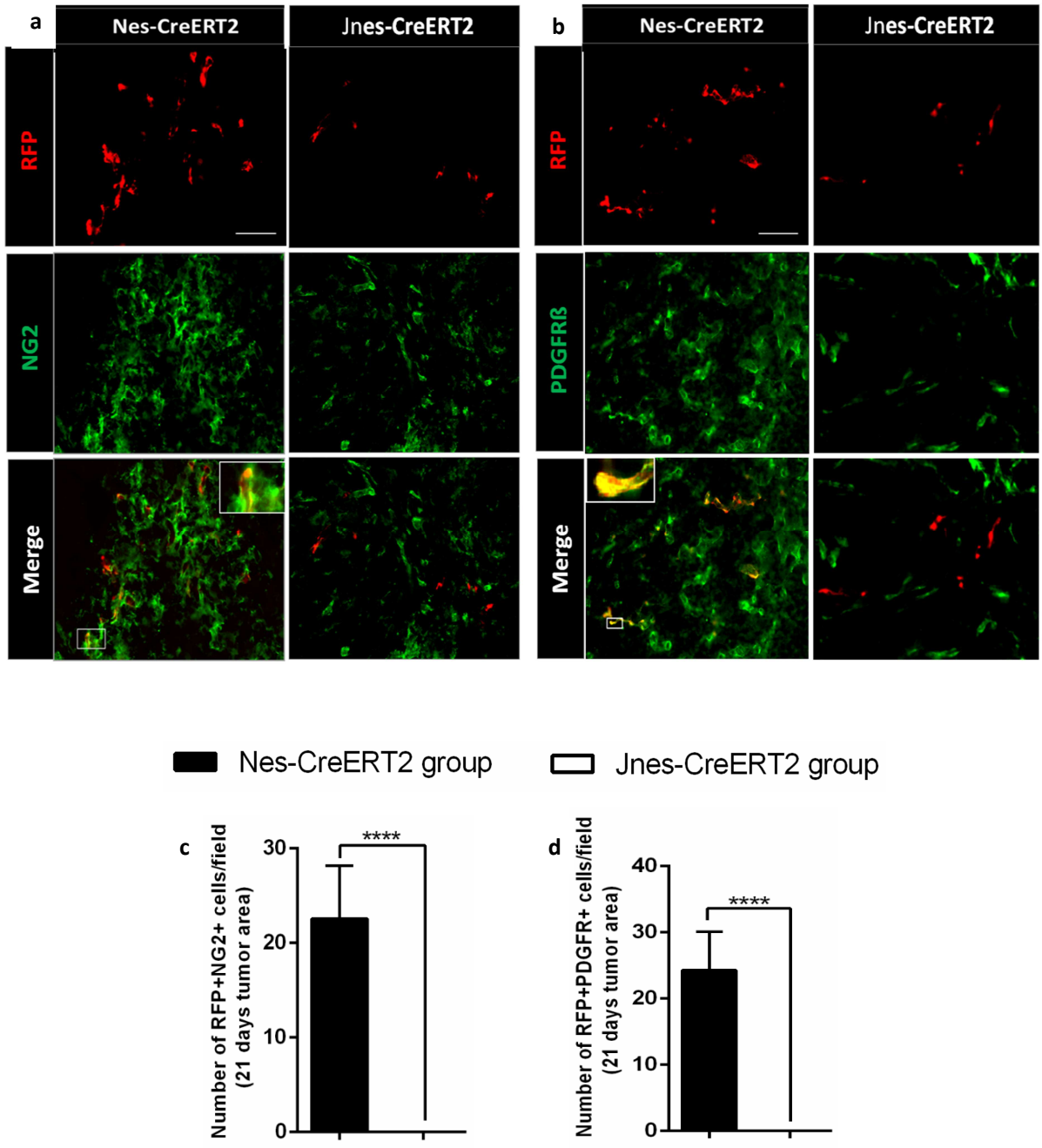

Figure 4.3.2 NG2 and PDGFRß expression in the NesCreER^{T2}-tdTomato and JnesCreER^{T2}-tdTomato mouse models

a-b: RFP (shown in red) and NG2 or PDGFRß (shown in green) expression in the tumor area of mouse brain samples from NesCreER^{T2} or JnesCreER^{T2} group (21 days tumor growth); **c-d:** RFP&NG2 or RFP&PDGFRß double positive cells in the tumor area were quantified from both groups, there was no RFP positive cells co-localized with NG2 or PDGFRß in JnesCreER^{T2} mouse group. Scale bars in **a,b,** 200μm.

4.3.3 GFAP expression in the NesCreER^{T2}-tdTomato and JnesCreER^{T2}-tdTomato mouse models

To investigate the fate of cells traced by the JnesCreER^{T2}-tdTomato mouse model, another series of immunohistochemical experiments was performed. Here it was observed that RFP-expressing cells in the JnesCreER^{T2} mouse strain co-localized with glial fibrillary acidic protein (GFAP). GFAP is an intermediate filament protein which is expressed by astrocytes in the central nervous system [56, 57]. GFAP positive cells play an important role in many processes of central neural system, such as the formation of blood brain barrier and cell communication [58]. GFAP expression in the peritumoral area was much higher than in the tumor area (Figure 4.3.3 a), RFP positive cells as well as RFP&GFAP double positive cells were quantified both in the tumor area and peritumoral area (Figure 4.3.3 b). Comparing the percentage of RFP&GFAP double positive cells accounting for RFP positive cells between tumor area and peritumoral area, there is a small but significant increase of the percentage of RFP&GFAP double positive cells in peritumor area (Figure 4.3.3 c, $p<0.05$).

Immunostaining for GFAP was also performed in NesCreER^{T2}-tdTomato mouse brain samples, similar to the JnesCreER^{T2} mouse group, GFAP expression was also detected mostly surrounding the tumor area (Figure 4.3.3 d). Unlike the JnesCreER^{T2} mouse model, there were almost no RFP positive cells co-localized with GFAP both in the tumor area or peritumoral area (Figure 4.3.3 e)，and there was a significant difference of the percentage of RFP&GFAP double positive cells as compared to JnesCreER^{T2} mouse group both in the tumor area or peritumoral area (Figure 4.3.3 f, g, $p<0.001$).

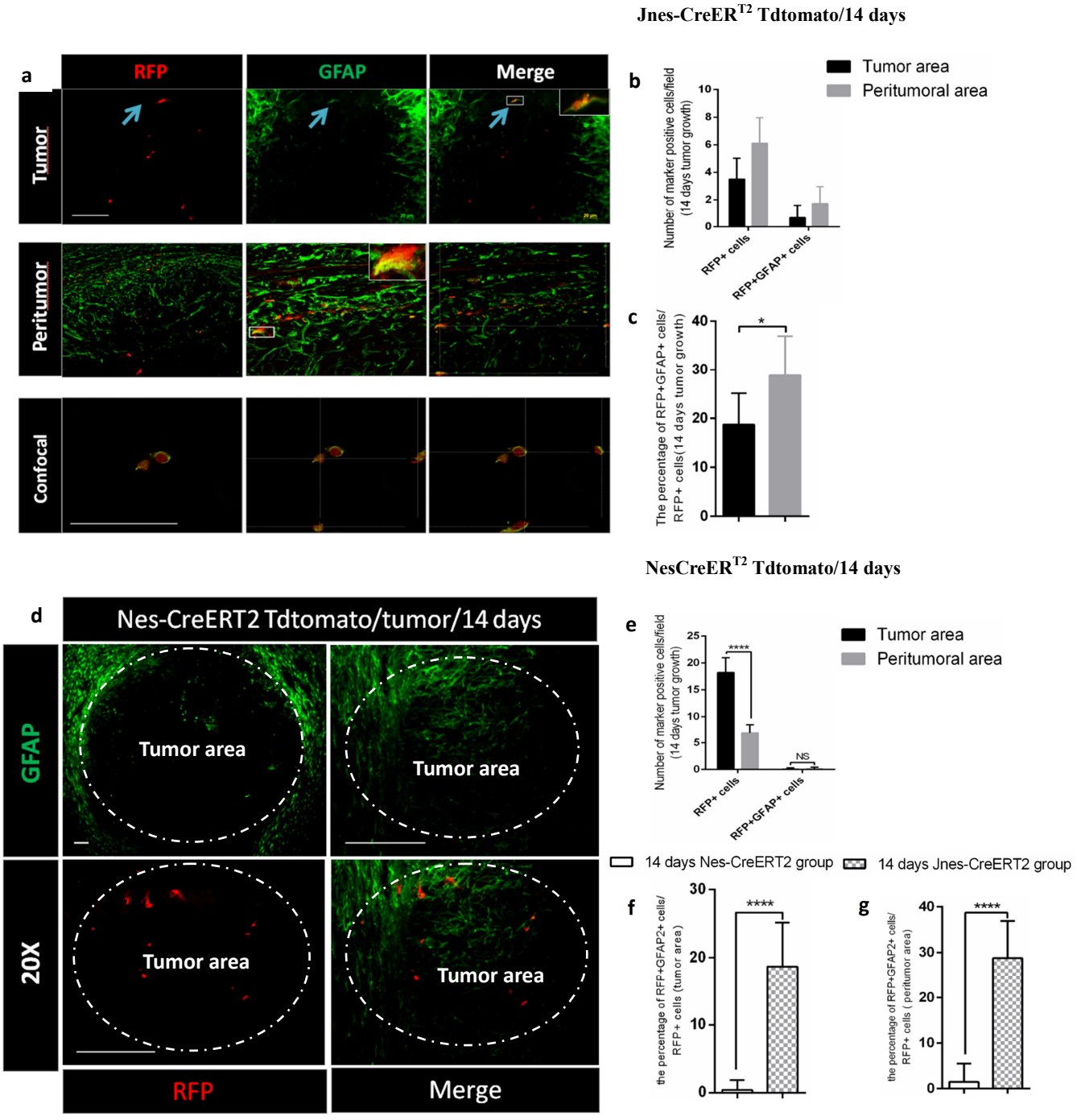

Figure 4.3.3 GFAP expression in the NesCreER^{T2}-tdTomato and JnesCreER^{T2} -tdTomato mouse models

a,d. RFP (shown in red) or GFAP (shown in green) expression in tumor area of mouse brain samples from NesCreER^{T2} and JnesCreER^{T2} groups (14 days); **b,e.** RFP positive cells and RFP&GFAP double positive cells were quantified from both groups; **f-g**. The percentage of RFP&GFAP double positive cells in JnesCreER^{T2} group is significantly higher than NesCreER^{T2} group both in tumor area and peritumoral area ($P<0.001$). Scale bars in **a,d,** 200μm, 300μm.

4.4 Immunohistochemical characterization of cells traced in the NesCreER^{T2}-tdTomato mouse model in a postnatal development

To further investigate the lineage of nestin positive cells in the NesCreERT2-tdTomato mouse strain, gene recombination was induced after birth (at postnatal day 0; P0), and the mice were sacrificed after 3 weeks (p21). The brain tissues were harvested for immunohistochemical analysis.

4.4.1 RFP expression in the NesCreER^{T2} Tdtomato mouse model in the postnatal brain

RFP positive cells were quantified in the cortex, striatum and brain stem (Fig 4.4.1 a). When comparing the numbers of RFP-positive cells in these 3 brain areas no difference was detected (Figure 4.4.1 b). The morphology of the RFP positive cells was heterogeneous; the majority displayed a vascular, pericyte-like morphology, indicating that they may develop into pericytes.

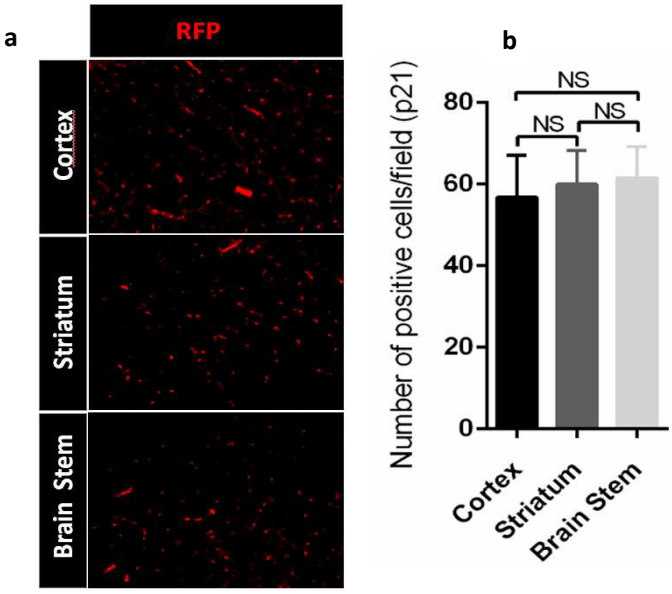

Figure 4.4.1 RFP expression in the NesCreER^{T2}-tdTomato pups (P 21)

a. RFP (shown in red) expression in the brain (cortex, striatum and brain stem) of NesCreERT2-tdTomato pups; **b.** RFP positive cells were quantified from cortex, striatum and brain stem, there was no difference in the number of RFP positive cells among the 3 areas.

4.4.2 Perivascular location of RFP-positive cells

To investigate if the traced cells acquired a perivascular-cell fate, immunofluorescence labelling for Von Willebrand factor (VWF), a blood glycoprotein that is considered to be important for hemostasis and represents a specific markers for endothelial cells [59] was performed. Staining with Isolectin-B4 (IB4) which can be used to label endothelial cells, microglia and macrophages was carried out. Most RFP-expressing cells were located near vascular structures (Figure 4.4.2). Staining with the pericyte marker PDGFRß showed that RFP-expressing cells located close to blood vessels and co-localized with PDGFRß (Figure 4.4.3), which indicated that the cells traced with the NesCreERT2-tdTomato mouse model over a postnatal period develop into pericytes. Importantly, this indicates that the NesCreERT2-tdTomato strain is a useful model to trace the pericyte lineage both in pathological neoangiogenesis during glioma growth and in physiological postnatal angiogenesis.

a

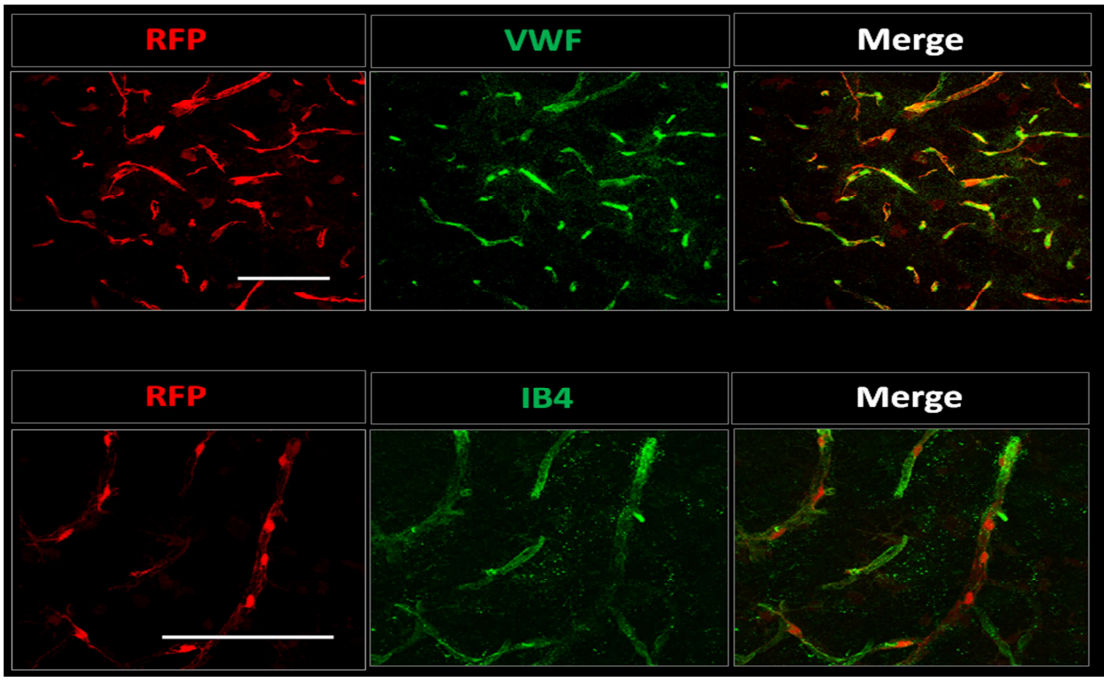

Figure4.4.2 Vascular markers (VWF and IB4) expression in the NesCreERT2-tdtomato postnatal mouse brain (P 21).

a. RFP (shown in red) and vascular markers VWF and IB4 (shown in green) expression in NesCreERT2-tdTomato postnatal mouse brain (P21); Scale bars in **a,** 50µm.

4.4.3 Investigating the fate of RFP-positive cells in the NesCreER^{T2}-tdTomato mouse model in postnatal brain development

The morphology and location of RFP-positive cells indicated that there is genesis of pericytes from the nestin positive linage. The mouse brain samples were stained with pericyte markers such as NG2, PDGFRß or desmin, and the analysis of co-localization of RFP positive cells with the pericyte markers was performed by confocal microscopy.

The data showed that at the postnatal day 21 (P21) many RFP-expressing cells expressed PDGFRß (Figure 4.4.3 a), confocal image analysis showed that RFP positive cells co-localized with PDGFRß (Figure 4.4.3b). The numbers of RFP positive cells and RFP&PDGFRß double positive cells were quantified (Figure 4.4.3 c), and the percentage of RFP&PDGFRß double positive cells accounting for total RFP positive cells was around 30% (Figure 4.4.3 d). Comparing the percentage of RFP&PDGFRß double positive cells in cortex, striatum and brain stem, there is a slight increase for the percentage of RFP&PDGFRß double positive cells in cortex, and there was no difference for the percentage between striatum and brain stem ($p>0.05$, Figure 4.4.3 e). Immunostainings for desmin and NG2 were also performed. The result showed that PDGFRß expression in the brain is significantly higher than the expression of desmin or NG2 ($p<0.01$, Figure 4.4.3 f). These findings indicated that many cells traced in the NesCreERT2-tdTomato mouse model at postnatal time point (P21) develop into pericytes.

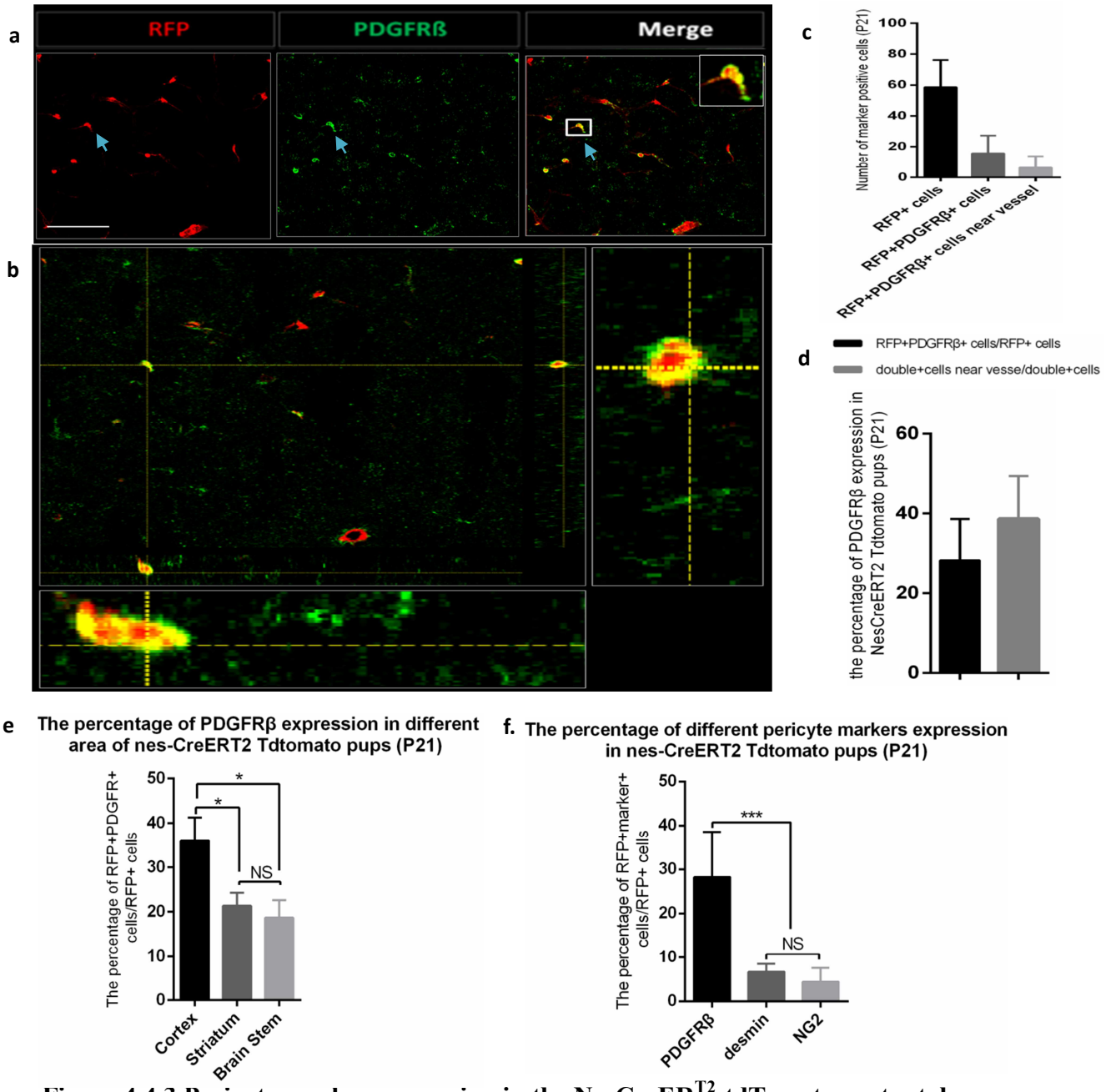

Figure 4.4.3 Pericyte marker expression in the NesCreER^{T2}-tdTomato postnatal mouse brain (P21).

a. RFP (shown in red) and PDGFRß (shown in green) expression in mouse brain samples from NesCreER^{T2}-Tdtomato pups (P21); **b.** Pictures from confocal microscopy indicated that PDGFRß co-localized with RFP-expressing cells; **c-d.** RFP positive cells and RFP&PDGFRß double positive cells were quantified; **e**. The percentage of PDGFRß expression in different area of the brain in nes-CreER^{T2} Tdtomato postnatal mice (P21) was calculated, the expression of PDGFRß in cortex is slightly higher than striatum or brain stem ($0.01p<0.05$); **f.** The percentage of different pericyte markers expression in the brain of nes-CreER^{T2} Tdtomato postnatal mice (P21) was calculated, at the same time point, the expression of PDGFRß is much more abundant in RFP positive cells than NG2 or desmin ($P<0.01$). Scale bar in **a,** 100μm.

4.4.4 Myeloid marker investigation

As shown above, the RFP positive cells expressed pericyte markers during postnatal brain development, some previous research suggested that microglia may derive from pericytes in the brain, for example, Monteiro et al demonstrated that microglia may derive from pericytes in rat cerebellar cortex [60]. In order to investigate whether the RFP positive cells express the myeloid lineage markers, Iba1 immunofluorescence staining was performed. As shown in Figure 4.4.4, there are no RFP positive cells co-localized with Iba1, indicating that in our study the RFP-positive pericytes do not develop into microglia.

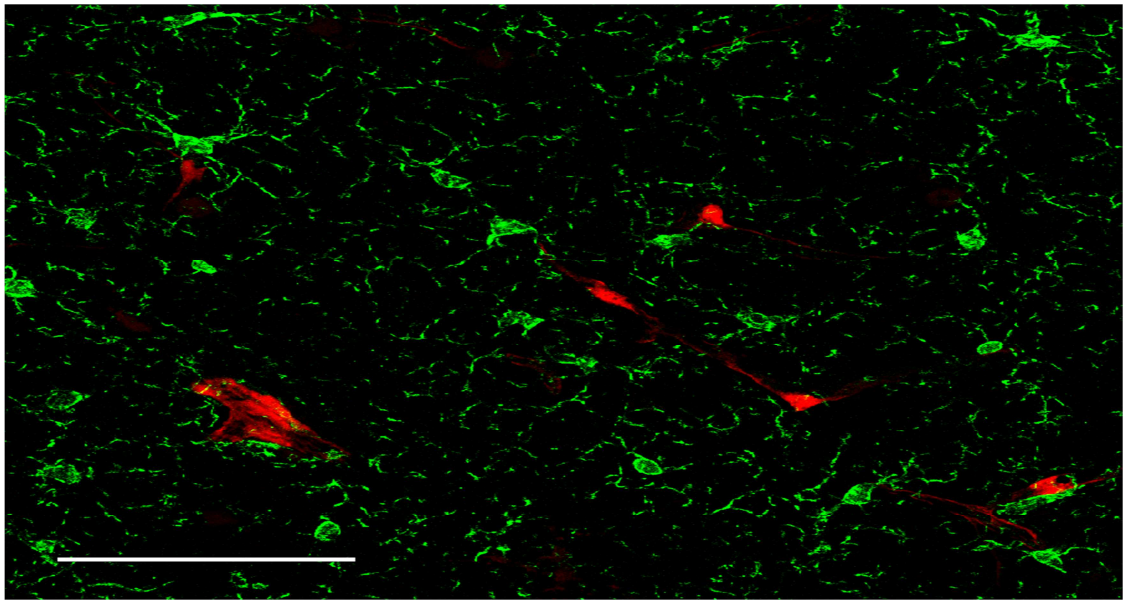

Figure4.4.4 Iba1 expression in the NesCreER^{T2}-tdtomato postnatal mouse brain (P 21).

RFP (shown in red) and Iba1 (shown in green) expression in the NesCreERT2-tdTomato postnatal mouse brain (P 21), there is no RFP positive cells co-localized with Iba1. Scale bar, 50μm.

4.4.5 Glial marker investigation in the pericyte-reporter mouse model

To investigate whether the traced cells develop into glial cells, immunofluorescence staining for GFAP was performed and subsequently samples were analyzed by confocal laser scanning microscopy. This staining showed that the RFP positive cells do not express GFAP, but are in close apposition to perivascular astrocytes.

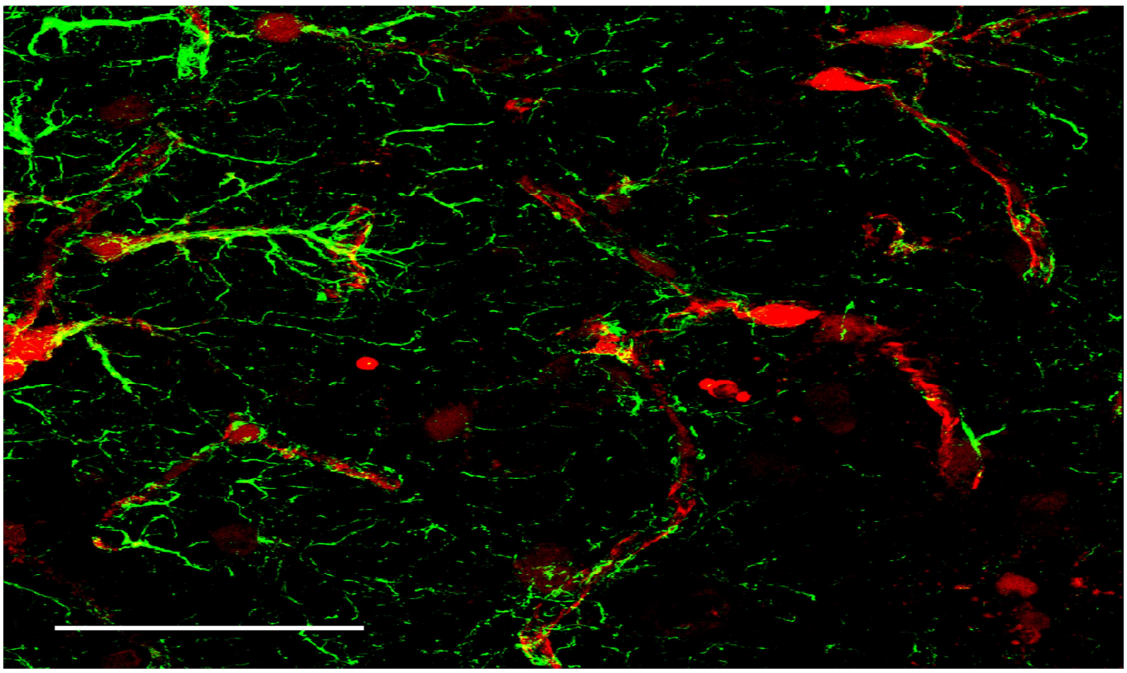

Figure4.4.5 GFAP expression in the NesCreER^{T2}-tdtomato postnatal mouse brain (P 21).

RFP (shown in red) and GFAP (shown in green) expression in the NesCreERT2-tdTomato postnatal mouse brain (P 21), there are no RFP positive cells co-localized with GFAP. Scale bar, 50µm.

4.4.6 RFP positive cells develop into pericytes of the retina in physiological condition

In our study the fate of RFP positive cells in retina was also traced in the NesCreERT2-tdTomato postnatal mice. At postnatal day 21, the pericytes were detected in the developing retina vasculature (Fig. a, b, the brown arrow). Immunostainings for the pericyte marker NG2 and the endothelial cell marker CD31 were performed (Fig. c, d), which showed that the RFP positive cells co-localized with NG2 and were located in a perivascular position, indicating that the RFP positive cells develop into pericytes of the retina under physiological condition.

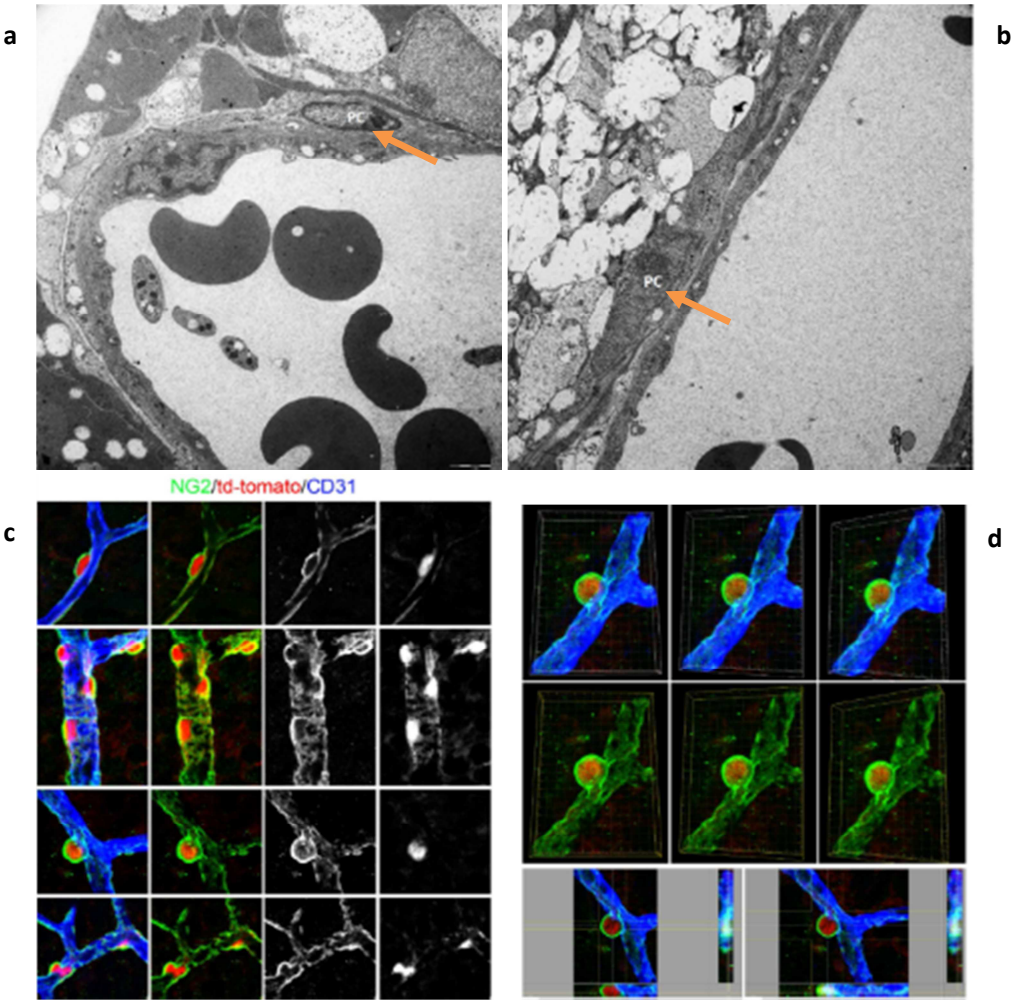

Fig.4.4.6 Vascular development in the retina.

a-b. pericytes (PC, the brown arrow) were shown in the ultrastructure of the developing retina vasculature; **c-d.** RFP (shown in red), NG2 (shown in green) and CD31 (shown in blue) expression in mouse retina from NesCreER^{T2}-Tdtomato pups (P21), the RFP positive cells co-localized with pericyte marker NG2 and located in a perivascular position.

5. Discussion

In this study we established a GL261 high-grade glioma mouse model in immune competent transgenic Nes-CreER^{T2} Tdtomato mice that allowed tracing the fate of nestin-expressing cells. We chose the GL261 mouse glioma model because it is syngeneic with the transgenic mouse model used in this study and faithfully recapitulate some pathological relevant features of GBM [61]. During the intracranial tumor growth, a significant increase in the number of RFP positive cells was observed and these RFP-positive cells co-localized with different pericyte markers (such as NG2, desmin, PDGFRß and CD146). After 7 days of tumor progression, few RFP-positive cells co-localized with pericye marker, whereas after 21 days of tumor growth most of the RFP-positive cells were immunofluorescently labelled with pericyte markers, which indicated that the pericyte progenitor cells (RFP positive and pericyte marker negative cells) developed into mature pericytes (RFP positive and pericyte marker positive cells) during the tumor expansion. The accumulation of new pericytes was most abundant within the tumor, but not in the peritumoral area or contralateral hemisphere, indicating that new pericytes derive from pericyte progenitor cells of the adult brain mainly during neo-angiogenesis. In another transgenic mouse model with a genetically different nestin construct (Jnes-CreER^{T2}Tdtomato mouse), we also traced intratumoral cells and these cells were found to express astrocyte markers like GFAP but not pericyte markers. Overall, our study shows that pericytes play an important role in brain tumor angiogenesis, and confirms that pericyte can provide a new target for anti-angiogenesis in brain cancer.

In our study we also used the transgenic Nes-CreER^{T2}Tdtomato mouse model to trace the fate of nestin-expressing cells in the tumor-free brain over postnatal period. We found that the traced cells distributed in the entire brain, many of which displayed a perivascular morphology and also expressed pericytes markers in the brain and retina (during an observation period of 21 days), indicating that the pericyte-progenitor cells marked by nestin-creER^{T2} mouse strain specifically trace brain-pericytes. This suggests an important physiological role of pericyte progenitors in brain development.

5.1 The pericyte progenitor cell

Pericytes play an important role in angiogenesis, but the origin of pericytes is still poorly understood. Some previous studies claimed the identification of a pericyte progenitor cell type, for example Steven Song et al showed that tumor derived PDGFRß+ perivascular progenitor cells have the ability to develop into pericytes in pancreatic carcinoma and a subset of PDGFRß+ pericyte progenitor cells are recruited from the bone marrow [62]. In this study a PDGFRß, desmin, NG2 and CD146 negative pericyte progenitor cell type was uncovered in glioma angiogenesis. Therefore, we established a GL261 high-grade glioma mouse model in transgenic Nes-CreER^{T2} Tdtomato mice to trace the fate of nestin-expressing cells and their progeny in the mouse brain. During the intracranial tumor growth, a significant increase in the number of RFP positive cells was observed. In the early time course (7 days of tumor growth) few RFP-positive cells co-localized with pericye markers,

whereas in the later time course (21 days of tumor growth) most of the RFP-positive cells expressed pericyte markers like PDGFRß, desmin, NG2 and CD146. These findings indicated that pericyte progenitor cells (RFP positive and pericyte marker negative cells) differentiated into mature pericytes (RFP positive and pericyte marker positive cells) during tumor expansion. These date showed that the new pericytes in glioma derived from pericyte progenitor cells (defined as RFP positive and pericyte marker negative cells) in the Nes-CreER^{T2} Tdtomato mouse model. In another transgenic mouse model with a different transgenic nestin-promoter element called JnesCreER^{T2} Tdtomato mouse model, we also traced the intratumoral RFP positive cells and these cells were found to express astrocyte markers like GFAP but not pericyte markers. Neural stem cells are capable of differentiating into astrocytes, neurons and oligodendroglia cells [63, 64], which indicates that the traced cells in JnesCreER^{T2} Tdtomato mouse model originate from neural stem cells. Taken together, the traced cells in Nes-CreER^{T2} Tdtomato mouse model express pericyte markers but not GFAP, indicating that the traced cells are pericyte progenitor cells; while the traced cells in JnesCreER^{T2} Tdtomato mouse model express GFAP but not pericyte markers, indicating that the traced cells derive from neural stem cells.

5.2 The role of pericytes in glioblastoma

Our findings from the Nes-CreER^{T2}-Tdtomato mouse model showed that new pericytes were accumulated specifically within the intracranial glioma, indicating that pericytes play an important role in brain tumor angiogenesis. As introduced before, the different functions of pericytes include maintenance of the BBB/Blood-Retina -Barrier (BRB), vessel-formation and vessel-maturation, angiogenesis and contractile function. Pericytes were considered as an important component of the glioblastoma vasculature, the tumor pericytes are able to facilitate tumor growth by promoting endothelial cell survival [65, 66] and mediating immunosuppression [67]. The origin of pericytes in glioblastoma is still a controversial issue. It was suggested that glioblastoma stem cells within the tumor itself generated the majority of new pericytes [68] or the pericytes in the tumor were derived from the bone marrow [69]. Furthermore, Daniel Bexell et al demonstrated that bone marrow–derived mesenchymal stromal cells (MSCs) share characteristics of pericytes in GBMs such as a strong tumor tropism, expression of pericyte markers (SMA, NG2 or PDGFRß) and integration into the tumor vessel wall [70]. In our study we showed that the pericyte progenitor cells differentiated into pericytes during the tumor expansion, the accumulation of new pericytes was observed mainly within the tumor, but not in the peritumoral area or contralateral hemisphere. Surprisingly, those newly formed pericytes appear to originate from a pericyte progenitor cell-type that may be endogenous to the brain as no td-Tomato positive cells were found in other organs (not shown).

Though previous research defined many molecular regulators which are important for pericyte activation and function [71], the mechanism of pericytes activation and recruitment after local tumor growth is not yet fully elucidated. There is a series of pathological alterations in the microenvironment of the brain throughout tumor growth, including the formation of hypoxic areas, edema and strong angiogenesis with many vascular malformations [33, 72, 73]. During glioma expansion more and more new pericytes will be recruited to participate in the formation of new vessels and play a crucial role in glioma angiogenesis.

Glioblastomas (GBMs) are highly aggressive tumors and rich in blood vessels, which can also provide a path for tumor invasion [74]. The major anti-angiogenic therapies for GBMs focus on targeting endothelial cells alone by blocking vascular endothelial growth factor (VEGF) signaling. However, though current anti-VEGF therapies are beneficial for some patients with cancer, VEGF-blockade does not improve overall survival of GBM patients [75]. Furthermore, anti-angiogenic therapies have the potential to trigger a more aggressive and metastatic phenotype in GBMs [76, 77], suggesting that anti-angiogenic therapy of targeting endothelial cells alone is not sufficient to control tumor progression effectively. In addition to endothelial cells, Pericytes are also an important component of tumor vessels [78]. Pericytes interact with endothelial cells and both control tumor vessel growth and integrity [79]. Moreover, pericytes can promote the resistance to anti-VEGF therapies by activating the PDGF receptor signaling pathway to protect the endothelial cells [77, 80].

Therefore, pericytes can provide a new target for anti-angiogenesis in brain cancer, and targeting endothelial cells and pericytes simultaneously might make anti-angiogenic therapy more effective.

5.3 The role of pericytes in vascular development of the retina

In our study RFP-expressing pericyte marker positive cells were not only detected in glioma-induced angiogenesis in the adult brain, but also in the postnatal mouse retina, indicating that RFP-traced pericytes play an important role in both physiological and pathological angiogenesis. The density of pericyte changes from organ to organ, it is reported that the highest relative ratio of pericytes to endothelial cells is detected in the retina and the brain, where the endothelial cell to pericyte ratio is 1:1, while it is often much lower in peripheral organs (like 1:100) [24, 81]. The arteries and arterioles of the retina are covered by vascular smooth muscle cells (vSMCs), whereas capillaries of the retina are covered by pericytes [82]. In the last two decades, pericytes were considered to be a primary component of the BRB. The BRB consists of the inner BRB (provided by the retinal vascular endothelium) and the outer BRB (which consists of retinal pigment epithelium) [82, 83]. Like the BBB, the BRB is a highly efficient regulated barrier, it can prevent the entry of potentially harmful substances to the CNS and guards the homeostasis of the neuronal microenvironment [84]. Though the structure of the Blood-Brain-Barrier is similar to the inner BRB [85], some studies showed that between brain and the neurovascular unit of the retina there is heterogeneity in transport properties [86]. Up to now, many studies have shown that

pericyte loss results in BBB breakdown and increases vascular permeability: by establishing a mouse model with PDGFRß signaling deficiency , Bell et al demonstrated that after reducing the coverage of pericytes in the brain, the BBB was damaged and a lot of plasma derived proteins accumulated in the CNS, finally leading to secondary neuronal degenerative alterations [33].There were also some studies that investigated the changes in neuronal function and BRB permeability under conditions when pericyte coverage was reduced. After endothelium-specific platelet-derived growth factor-B ablation mice, Enge et al demonstrated that reduced pericyte coverage in capillaries led to a fast pathologic progression in diabetic retinopathy [43]. Furthermore, pericytes can promote the formation of tight junctions in developing retinal vasculature in postnatal mice [87].

A reduced vessel coverage and altered function of pericytes can be causally involved in certain CNS diseases [88]. Diabetes mellitus refers to a group of metabolic diseases and diabetic retinopathy (DR) is one major complication. The characterization of DR includes progressive vascular occlusion, Blood-Retina-Barrier breakdown, increased vascular permeability and neuronal damage finally leading to a serious visual impairment [89]. Though during the pathologic progression of DR pericyte loss is considered as a well-established fact, the potential mechanisms of DR is still not clear [90]. Pericyte loss through apoptosis has been suggested, which is associated with hyperglycemic conditions, neuro inflammation, reduced trophic factor signaling, oxidative stress and glutamate receptor excitation [91, 92]. Up to now, substantial research has been devoted to investigating the underlying mechanisms of vascular

leakage and pericyte loss in DR, but the reasons for BRB breakdown still remain unclear [43, 93]. In summary, pericytes play an indispensable role in the formation and the stability of BRB, pericyte deficiency leads to pathological progression of diverse CNS diseases, pericytes can provide a promising target for regenerative therapeutic approaches in the future.

6. Summary

The current study established that a transgenic mouse model, Nes-CreER^{T2} Tdtomato, is of use to trace the fate of nestin-expressing cells in glioma progression and postnatal brain development. Through a series of cell type identification tests, using immunofluorescence labelling and confocal microscopy, it was shown that these nestin-positive cells generate new pericytes, but initially do not have a pericyte identity, this is corroborated by the following findings:

(1) In the Nes-CreER^{T2} Tdtomato mouse model, the number of traced cells (RFP positive cells) increased during the intracranial tumor growth. At an early time point (7 days) few of the RFP positive cells co-localized with pericyte markers while at a later time point (21 days) most of the RFP positive cells co-localized with pericyte markers, which indicated that the new pericytes in glioma derived from the pericyte progenitor cells (defined as RFP positive and pericyte marker negative cells) in the Nes-CreER^{T2} Tdtomato mouse model;

(2) In the JnesCreER^{T2} Tdtomato mouse model, the traced cells were found to express astrocyte-markers like GFAP but not pericyte markers, which indicated that the traced cells in the JnesCreER^{T2} Tdtomato mouse model were originally neural stem cells rather than pericyte progenitor cells. Hence, only the Nes-CreER^{T2} Tdtomato mouse model is useful to study pericyte development in the brain.

(3) The cells traced with the NesCreERT2-tdTomato mouse model over a postnatal

period develop into pericytes in the brain, which indicates that the NesCreERT2-tdTomato strain is a useful model to trace the pericyte lineage both in pathological neoangiogenesis during glioma growth and in physiological postnatal angiogenesis.

(4) In this study RFP-expressing pericyte marker positive cells were detected in the postnatal mouse retina, indicating that RFP-traced pericytes play an important role in both pathological angiogenesis and physiological vascular development of retina.

Zusammenfassung

Die vorliegende Doktorarbeit zeigt, dass das NesCreERT2 TdTomato Maus Modell verwendet werden kann, um ein Lineage-Tracing von Zellen aus der Nestin positiven Linie während des Gliom-Wachstums und der postnatalen ZNS-Entwicklung durchzuführen. Anhand einer Reihe von Zelltyp-Identifizierungs-Tests mithilfe von Immunfluoreszenz und Konfokalmikroskopie wurde gezeigt, dass sich diese Nestin-positiven Zellen zu neuen Perizyten entwickeln, allerdings initial keine Perizyten-Marker tragen. Dies wird durch folgende Ergebnisse verdeutlicht:

(1) Im NesCreERT2 TdTomato Maus Modell nahm die Anzahl der Zellen aus der Nestin positiven Linie (RFP positive Zellen) während des intrakraniellen Tumorwachstums zu. Zu einem frühen Zeitpunkt (7 Tage) co-lokalisierten wenige der RFP positiven Zellen mit Perizyten-Markern, während zu einem späteren Zeitpunkt (21 Tage) die meisten der RFP positiven Zellen mit Perizyten-Markern co-lokalisierten. Dies weist darauf hin, dass im NesCreERT2 TdTomato Maus Modell neue Perizyten innerhalb von Gliomen von Perizyten-Vorläufer-Zellen (definiert als RFP-positive und Perizyten-Marker-negative Zellen) abstammen.

(2) Im JnesCreERT2 TdTomato Maus Modell exprimierten die Zellen aus der Nestin positiven Linie Astrozyten-Marker wie beispielsweise GFAP, aber keine Perizyten-Marker, was darauf hindeutet, dass diese im JnesCreERT2 TdTomato Maus Modell ursprünglich Neuronale Stammzellen darstellten, allerdings keine

Perizyten-Vorläufer-Zellen. Entsprechend kann nur das NesCreERT2 TdTomato Maus Modell, nicht jedoch das JnesCreERT2 TdTomato Maus Modell, für eine Analyse der Perizyten-Entwicklung im zentralen Nervensystem verwendet werden.

(3) Im NesCreERT2 TdTomato Maus Modell entwickelten sich die Zellen aus der Nestin positiven Linie postnatal zu Perizyten im zentralen Nervensystem. Dies deutet darauf hin, dass besagtes Maus Modell für ein Lineage-Tracing von Perizyten verwendet werden kann, sowohl während pathologischer Neoangiogenese im Kontext des Gliom-Wachstums als auch während physiologischer postnataler Angiogenese.

(4) Im Rahmen der vorliegenden Arbeit wurden RFP-exprimierende, Perizyten-Marker-positive Zellen in postnatalem, murinen Retinagewebe gefunden, was verdeutlicht, dass RFP-positive Perizyten sowohl bei pathologischer Angiogenese als auch bei der physiologischen Vaskularisierung der Retina eine wichtige Rolle spielen.

7. References

1. Mamelak, A.N. and D.B. Jacoby, *Targeted delivery of antitumoral therapy to glioma and other malignancies with synthetic chlorotoxin (TM-601).* Expert Opin Drug Deliv, 2007. **4**(2): p. 175-86.
2. Goodenberger, M.L. and R.B. Jenkins, *Genetics of adult glioma.* Cancer Genet, 2012. **205**(12): p. 613-21.
3. Louis, D.N., et al., *The 2007 WHO classification of tumours of the central nervous system.* Acta Neuropathol, 2007. **114**(2): p. 97-109.
4. Stupp, R., et al., *Effects of radiotherapy with concomitant and adjuvant temozolomide versus radiotherapy alone on survival in glioblastoma in a randomised phase III study: 5-year analysis of the EORTC-NCIC trial.* Lancet Oncol, 2009. **10**(5): p. 459-66.
5. Taylor, L.P., *Diagnosis, treatment, and prognosis of glioma: Five new things.* Neurology, 2010. **75**(1): p. 28-32.
6. Ostrom, Q.T., et al., *CBTRUS statistical report: primary brain and central nervous system tumors diagnosed in the United States in 2007-2011.* Neuro Oncol, 2014. **16 Suppl 4**: p. iv1-63.
7. Roy, S., et al., *Recurrent Glioblastoma: Where we stand.* South Asian J Cancer, 2015. **4**(4): p. 163-73.
8. Davis, F.G., et al., *Survival rates in patients with primary malignant brain tumors stratified by patient age and tumor histological type: an analysis based on Surveillance, Epidemiology, and End Results (SEER) data, 1973-1991.* J Neurosurg, 1998. **88**(1): p. 1-10.
9. McLendon, R.E. and E.C. Halperin, *Is the long-term survival of patients with intracranial glioblastoma multiforme overstated?* Cancer, 2003. **98**(8): p. 1745-8.
10. Scott, J.N., et al., *Long-term glioblastoma multiforme survivors: a population-based study.* Can J Neurol Sci, 1998. **25**(3): p. 197-201.
11. Yoshida, T., et al., *Clinical cure of glioblastoma--two case reports.* Neurol Med Chir (Tokyo), 2000. **40**(4): p. 224-9.
12. Omuro, A. and L.M. DeAngelis, *Glioblastoma and other malignant gliomas: a clinical review.* Jama, 2013. **310**(17): p. 1842-50.

13. Stupp, R., et al., *Radiotherapy plus concomitant and adjuvant temozolomide for glioblastoma.* N Engl J Med, 2005. **352**(10): p. 987-96.

14. Friedman, H.S., et al., *Bevacizumab alone and in combination with irinotecan in recurrent glioblastoma.* J Clin Oncol, 2009. **27**(28): p. 4733-40.

15. Kreisl, T.N., et al., *Phase II trial of single-agent bevacizumab followed by bevacizumab plus irinotecan at tumor progression in recurrent glioblastoma.* J Clin Oncol, 2009. **27**(5): p. 740-5.

16. Glass, R. and M. Synowitz, *CNS macrophages and peripheral myeloid cells in brain tumours.* Acta Neuropathol, 2014. **128**(3): p. 347-62.

17. Brennan, C.W., et al., *The somatic genomic landscape of glioblastoma.* Cell, 2013. **155**(2): p. 462-77.

18. Phillips, H.S., et al., *Molecular subclasses of high-grade glioma predict prognosis, delineate a pattern of disease progression, and resemble stages in neurogenesis.* Cancer Cell, 2006. **9**(3): p. 157-73.

19. van Dijk, C.G., et al., *The complex mural cell: pericyte function in health and disease.* Int J Cardiol, 2015. **190**: p. 75-89.

20. Gaengel, K., et al., *Endothelial-Mural Cell Signaling in Vascular Development and Angiogenesis.* Arteriosclerosis Thrombosis & Vascular Biology, 2009. **29**(5): p. 630-638.

21. Etchevers, H.C., et al., *The cephalic neural crest provides pericytes and smooth muscle cells to all blood vessels of the face and forebrain.* Development, 2001. **128**(7): p. 1059-68.

22. Mandarino, L.J., et al., *Regulation of fibronectin and laminin synthesis by retinal capillary endothelial cells and pericytes in vitro.* Exp Eye Res, 1993. **57**(5): p. 609-21.

23. Sims, D.E., *Diversity within pericytes.* Clin Exp Pharmacol Physiol, 2000. **27**(10): p. 842-6.

24. Mathiisen, T.M., et al., *The perivascular astroglial sheath provides a complete covering of the brain microvessels: an electron microscopic 3D reconstruction.* Glia, 2010. **58**(9): p. 1094-103.

25. Shepro, D. and N.M. Morel, *Pericyte physiology.* Faseb j, 1993. **7**(11): p. 1031-8.

26. Armulik, A., G. Genove, and C. Betsholtz, *Pericytes: developmental, physiological, and pathological perspectives, problems, and promises.* Dev Cell, 2011. **21**(2): p. 193-215.

27. Hall, A.P., *Review of the pericyte during angiogenesis and its role in cancer and diabetic retinopathy.* Toxicol Pathol, 2006. **34**(6): p. 763-75.

28. Ribatti, D., B. Nico, and E. Crivellato, *The role of pericytes in angiogenesis.* Int J Dev Biol, 2011.

55(3): p. 261-8.

29. Crisan, M., et al., *A perivascular origin for mesenchymal stem cells in multiple human organs.* Cell Stem Cell, 2008. **3**(3): p. 301-13.

30. Armulik, A., A. Abramsson, and C. Betsholtz, *Endothelial/pericyte interactions.* Circ Res, 2005. **97**(6): p. 512-23.

31. Sa-Pereira, I., D. Brites, and M.A. Brito, *Neurovascular unit: a focus on pericytes.* Mol Neurobiol, 2012. **45**(2): p. 327-47.

32. Daneman, R., et al., *Pericytes are required for blood-brain barrier integrity during embryogenesis.* Nature, 2010. **468**(7323): p. 562-6.

33. Bell, R.D., et al., *Pericytes control key neurovascular functions and neuronal phenotype in the adult brain and during brain aging.* Neuron, 2010. **68**(3): p. 409-27.

34. Armulik, A., et al., *Pericytes regulate the blood-brain barrier.* Nature, 2010. **468**(7323): p. 557-61.

35. Gerhardt, H. and C. Betsholtz, *Endothelial-pericyte interactions in angiogenesis.* Cell Tissue Res, 2003. **314**(1): p. 15-23.

36. Winkler, E.A., R.D. Bell, and B.V. Zlokovic, *Central nervous system pericytes in health and disease.* Nat Neurosci, 2011. **14**(11): p. 1398-405.

37. Betsholtz, C., *Insight into the physiological functions of PDGF through genetic studies in mice.* Cytokine Growth Factor Rev, 2004. **15**(4): p. 215-28.

38. Lindahl, P., et al., *Pericyte loss and microaneurysm formation in PDGF-B-deficient mice.* Science, 1997. **277**(5323): p. 242-5.

39. Hellstrom, M., et al., *Lack of pericytes leads to endothelial hyperplasia and abnormal vascular morphogenesis.* J Cell Biol, 2001. **153**(3): p. 543-53.

40. Soriano, P., *Abnormal kidney development and hematological disorders in PDGF beta-receptor mutant mice.* Genes Dev, 1994. **8**(16): p. 1888-96.

41. Leveen, P., et al., *Mice deficient for PDGF B show renal, cardiovascular, and hematological abnormalities.* Genes Dev, 1994. **8**(16): p. 1875-87.

42. Tallquist, M.D., W.J. French, and P. Soriano, *Additive effects of PDGF receptor beta signaling pathways in vascular smooth muscle cell development.* PLoS Biol, 2003. **1**(2): p. E52.

43. Enge, M., et al., *Endothelium-specific platelet-derived growth factor-B ablation mimics*

diabetic retinopathy. Embo j, 2002. **21**(16): p. 4307-16.

44. Bandopadhyay, R., et al., *Contractile proteins in pericytes at the blood-brain and blood-retinal barriers.* J Neurocytol, 2001. **30**(1): p. 35-44.

45. Fernandez-Klett, F., et al., *Pericytes in capillaries are contractile in vivo, but arterioles mediate functional hyperemia in the mouse brain.* Proc Natl Acad Sci U S A, 2010. **107**(51): p. 22290-5.

46. Allt, G. and J.G. Lawrenson, *Pericytes: cell biology and pathology.* Cells Tissues Organs, 2001. **169**(1): p. 1-11.

47. Rucker, H.K., H.J. Wynder, and W.E. Thomas, *Cellular mechanisms of CNS pericytes.* Brain Res Bull, 2000. **51**(5): p. 363-9.

48. Imayoshi, I., et al., *Temporal regulation of Cre recombinase activity in neural stem cells.* Genesis, 2006. **44**(5): p. 233-8.

49. Lendahl, U., L.B. Zimmerman, and R.D. McKay, *CNS stem cells express a new class of intermediate filament protein.* Cell, 1990. **60**(4): p. 585-95.

50. Feil, R., et al., *Regulation of Cre recombinase activity by mutated estrogen receptor ligand-binding domains.* Biochem Biophys Res Commun, 1997. **237**(3): p. 752-7.

51. Branda, C.S. and S.M. Dymecki, *Talking about a revolution: The impact of site-specific recombinases on genetic analyses in mice.* Dev Cell, 2004. **6**(1): p. 7-28.

52. Crisan, M., et al., *Perivascular cells for regenerative medicine.* J Cell Mol Med, 2012. **16**(12): p. 2851-60.

53. Ozerdem, U., et al., *NG2 proteoglycan is expressed exclusively by mural cells during vascular morphogenesis.* Dev Dyn, 2001. **222**(2): p. 218-27.

54. Imayoshi, I., M. Sakamoto, and R. Kageyama, *Genetic Methods to Identify and Manipulate Newly Born Neurons in the Adult Brain.* Frontiers in Neuroscience, 2011. **5**: p. 64.

55. Sun, M.Y., et al., *Specificity and efficiency of reporter expression in adult neural progenitors vary substantially among nestin-CreER T2 lines.* Journal of Comparative Neurology, 2014. **522**(5): p. 1191-208.

56. Jacque, C.M., et al., *Determination of glial fibrillary acidic protein (GFAP) in human brain tumors.* J Neurol Sci, 1978. **35**(1): p. 147-55.

57. Venkatesh, K., et al., *In vitro differentiation of cultured human CD34+ cells into astrocytes.* Neurol India, 2013. **61**(4): p. 383-8.

58. Liedtke, W., et al., *GFAP is necessary for the integrity of CNS white matter architecture and long-term maintenance of myelination.* Neuron, 1996. **17**(4): p. 607-15.

59. Sadler, J.E., *Biochemistry and genetics of von Willebrand factor.* Annu Rev Biochem, 1998. **67**: p. 395-424.

60. Monteiro, R.A., E. Rocha, and M.M. Marini-Abreu, *Do microglia arise from pericytes? An ultrastructural and distribution study in the rat cerebellar cortex.* Journal of Submicroscopic Cytology & Pathology, 1996. **28**(4): p. 457.

61. Newcomb, E.W. and D. Zagzag, *The Murine GL261 Glioma Experimental Model to Assess Novel Brain Tumor Treatments*. 2008. 227-241.

62. Song, S., et al., *PDGFRβ+ perivascular progenitor cells in tumours regulate pericyte differentiation and vascular survival.* Nature Cell Biology, 2005. **7**(9): p. 870-879.

63. Alvarezbuylla, A., J.M. Garcíaverdugo, and A.D. Tramontin, *A unified hypothesis on the lineage of neural stem cells.* Nature Reviews Neuroscience, 2001. **2**(4): p. 287-293.

64. Kageyama, R., J. Hatakeyama, and T. Ohtsuka, *Roles of Hes bHLH Factors in Neural Development*. 2006. 1-22.

65. Bergers, G., et al., *Benefits of targeting both pericytes and endothelial cells in the tumor vasculature with kinase inhibitors.* Journal of Clinical Investigation, 2003. **111**(9): p. 1287-95.

66. Franco, M., et al., *Pericytes promote endothelial cell survival through induction of autocrine VEGF-A signaling and Bcl-w expression.* Blood, 2011. **118**(10): p. 2906-17.

67. Ochs, K., et al., *Immature mesenchymal stem cell-like pericytes as mediators of immunosuppression in human malignant glioma.* Journal of Neuroimmunology, 2013. **265**(1-2): p. 106–116.

68. Cheng, L., et al., *Glioblastoma stem cells generate vascular pericytes to support vessel function and tumor growth.* Cell, 2013. **153**(1): p. 139–152.

69. Du, R., et al., *HIF1alpha induces the recruitment of bone marrow-derived vascular modulatory cells to regulate tumor angiogenesis and invasion.* Cancer Cell, 2008. **13**(3): p. 206-20.

70. Bexell, D., et al., *Bone Marrow Multipotent Mesenchymal Stroma Cells Act as Pericyte-like Migratory Vehicles in Experimental Gliomas.* Molecular Therapy the Journal of the American Society of Gene Therapy, 2009. **17**(1): p. 183-90.

71. Jr, D.F.L., et al., *Adult stem cells and repair through granulation tissue.* Frontiers in Bioscience,

2009. **14**(14): p. 1433-70.

72. Kucharzewska, P., et al., *Exosomes reflect the hypoxic status of glioma cells and mediate hypoxia-dependent activation of vascular cells during tumor development.* Proceedings of the National Academy of Sciences, 2013. **110**(18): p. 7312-7.

73. Castejón, O.J., *Ultrastructural pathology of cortical capillary pericytes in human traumatic brain oedema.* Folia Neuropathologica, 2011. **49**(3): p. 162.

74. Norden, A.D., J. Drappatz, and P.Y. Wen, *Antiangiogenic therapies for high-grade glioma.* Nature Reviews Neurology, 2009. **5**(11): p. 610-20.

75. Lombardi, G., et al., *Effectiveness of antiangiogenic drugs in glioblastoma patients: A systematic review and meta-analysis of randomized clinical trials.* Critical Reviews in Oncology/hematology, 2017. **111**: p. 94.

76. Pàez-Ribes, M., et al., *Antiangiogenic therapy elicits malignant progression of tumors to increased local invasion and distant metastasis.* Cancer Cell, 2009. **15**(3): p. 220-31.

77. Potente, M., H. Gerhardt, and P. Carmeliet, *Basic and therapeutic aspects of angiogenesis.* Cell, 2011. **146**(6): p. 873-87.

78. Bergers, G. and S. Song, *The role of pericytes in blood-vessel formation and maintenance.* Neuro-Oncology, 2005. **7**(4): p. 452-64.

79. Peter, C. and R.K. Jain, *Principles and mechanisms of vessel normalization for cancer and other angiogenic diseases.* Nature Reviews Drug Discovery, 2011. **10**(6): p. 417-27.

80. Liu, A.Y. and G. Ouyang, *Tumor angiogenesis: a new source of pericytes.* Current Biology Cb, 2013. **23**(13): p. 565-8.

81. Díazflores, L., et al., *Pericytes. Morphofunction, interactions and pathology in a quiescent and activated mesenchymal cell niche.* Histology & Histopathology, 2009. **24**(7): p. 909-69.

82. Pfister, F., et al., *Pericytes in the eye.* Pflügers Archiv - European Journal of Physiology, 2013. **465**(6): p. 789-796.

83. Vinores, S.A., *Assessment of blood-retina1 barrier integrity.* Histology & Histopathology, 1995. **10**(1): p. 141-154.

84. Trost, A., et al., *Brain and Retinal Pericytes: Origin, Function and Role.* Frontiers in Cellular Neuroscience, 2016. **10**: p. 20.

85. Hosoya, K., et al., *Roles of inner blood-retinal barrier organic anion transporter 3 in the*

vitreous/retina-to-blood efflux transport of p-aminohippuric acid, benzylpenicillin, and 6-mercaptopurine. Journal of Pharmacology & Experimental Therapeutics, 2009. **329**(1): p. 87-93.

86. Andre, P., et al., *Transport of biogenic amine neurotransmitters at the mouse blood-retina and blood-brain barriers by uptake1 and uptake2.* J Cereb Blood Flow Metab, 2012. **32**(11): p. 1989-2001.

87. Kim, J.H., et al., *Recruitment of pericytes and astrocytes is closely related to the formation of tight junction in developing retinal vessels.* Journal of Neuroscience Research, 2009. **87**(3): p. 653–659.

88. Lange, S., et al., *Brain pericyte plasticity as a potential drug target in CNS repair.* Drug Discovery Today, 2013. **18**(9–10): p. 456-463.

89. Hammes, H.P., et al., *Pericytes and the pathogenesis of diabetic retinopathy.* Diabetes, 2002. **51**(10): p. 3107-12.

90. Qian, H. and H. Ripps, *Neurovascular Interaction and the Pathophysiology of Diabetic Retinopathy.* Experimental Diabetes Research, 2011. **2011**(3): p. 1-1.

91. Behl, Y., et al., *Diabetes-enhanced tumor necrosis factor-alpha production promotes apoptosis and the loss of retinal microvascular cells in type 1 and type 2 models of diabetic retinopathy.* American Journal of Pathology, 2008. **172**(5): p. 1411-8.

92. Alistair J. Barber, T.W.G., Steven F. Abcouwer, *The Significance of Vascular and Neural Apoptosis to the Pathology of Diabetic Retinopathy.* Investigative Ophthalmology & Visual Science, 2011. **52**(2): p. 1156.

93. Huang, H., et al., *TNFα Is Required for Late BRB Breakdown in Diabetic Retinopathy, and Its Inhibition Prevents Leukostasis and Protects Vessels and Neurons from Apoptosis.* Investigative Ophthalmology & Visual Science, 2011. **52**(3): p. 1336-44.

8. Acknowledgement

Herein I would like to express my sincere and humble acknowledgements to all those who helped me during the working in lab and the writing of this thesis. Without their helps, I could not have believed that I can finish my experiments and doctor thesis successfully.

First, I would like to express my deepest gratitude to my supervisor: Prof. Rainer Glass, for his constant guidance and encouragement. From the time when I arrived in Munich, he gives me a great deal of help in learning and working, I also learned a lot with his help. Without his consistent instruction, my dissertation could not reach the present form.

Second, I would like to express my heartfelt gratitude to my co-supervisor Dr.Roland and other colleagues in our lab. Dr.Roland and Lange Stefanie teaches me many experimental methods and techniques, Dr. Eloi Montanez Miralles from Walter-Brendel-Center provided the retina date, and the electron microscope pictures were from the Department of Pathology at the Helmholtz Center, Munich. Yuping Li, Katharina Eisenhut, Marie Volmar, Ramazan Uyar, Giorgia Mastrella, Song Gu and Mengzhuo Hou, Min Li, Linzhi Cai all help me a lot in the past three years. They bring me a wonderful time in my life and I will keep in my heart forever.

Finally, I would like to express my thanks to my beloved family for their continued support and concern for so many years. And I am grateful to everyone who helped me during my difficult time.